Climate Dynamics (2023) 60:3435–3454
https://doi.org/10.1007/s00382-022-06517-5

Simulation of the potential impacts of lakes on glacier behavior over the Tibetan Plateau in summer

Dongsheng Su[1,2] · Lijuan Wen[1] · Anning Huang[3] · Yang Wu[3] · Xiaoqing Gao[1] · Mengxiao Wang[1] · Yixin Zhao[1] · Georgiy Kirillin[4]

Received: 13 April 2022 / Accepted: 19 September 2022 / Published online: 6 October 2022

Abstract
Known as "Asian Water Tower", the Tibetan Plateau (TP) contains the largest glacierized area outside the polar regions and contains more than half of China's lakes. However, these glaciers are retreating rapidly under the influence of global warming. Many studies have attempted to explain the spatial heterogeneity of glacier retreat in the TP and its impacts on local lakes, but few studies have focused on the feedback of lakes on glaciers, especially in summer with intense lake effects and glacier ablation. Using an air-lake coupled model, the potential summer climatic impacts of the lake clusters on glacier behavior over TP are investigated based on two experiments with and without the lakes. Away from the lake-rich area of Inner TP, glaciers along the Himalayas are retreating rapidly with climate warming. The most pronounced glacier ablation occurs in southeastern TP, where TP lakes reduce snowfall. However, in the Inner TP, the influence of climate warming on glaciers is partially offset by the lakes through different lake-related mechanisms. The glaciers on the Western Nyainqentanglha Range are preserved mainly by the local cooling and snowfall-increase caused by nearby Nam Co. In turn, the numerous small lakes in the Eastern Inner TP exert a cumulative effect on preserving the glaciers through cooling and moistening the atmospheric boundary layer and thus increasing snowfall. The glaciers in the western Kunlun Mountains benefit from the large-scale impacts of the TP lakes, which intensified westerlies and lead to regional temperature decrease and snowfall increase.

Keywords Tibetan Plateau · Lake · Climate effect · Glaciers · Regional climate modeling

1 Introduction

The Tibetan Plateau (TP), known as the "Third Pole" (Qiu 2008), is the highest and largest plateau in the world, with an average elevation of > 4000 m above sea level (a.s.l.). Lots of the highest mountains on earth are located here (Yao et al. 2012a), which results in cold, dry, and strongly insolated climatic conditions. There are almost 100,000 km^2 of glaciers in the TP and its neighboring areas, constituting the largest cryospheric region outside the Antarctic and Arctic (Yao et al. 2019). Meltwater from snow and glaciers feeds major Asian rivers, such as the Yangtze, Yellow, Brahmaputra, Ganges, and Indus, that provide water for drinking, irrigation, and hydropower for billions of inhabitants of the downstream plains (Huss et al. 2017; Immerzeel et al. 2020; Pritchard 2019; Qiu 2008). Therefore, understanding the change of glaciers and the associated issues is essential for human livelihood, society and economy.

Rising temperature and changing precipitation patterns are regarded as the primary drivers of glacier retreat and snow cover variations on the TP (Bibi et al. 2018; Wu et al. 2019a; Yang et al. 2019). During recent decades, the TP has experienced significant warming, which is much faster than global warming (Cai et al. 2017; Duan and Xiao 2015; Guo and Wang 2012; Kuang and Jiao 2016; Pepin et al. 2015; You et al. 2019). Herewith, a global

✉ Lijuan Wen
wlj@lzb.ac.cn

1 Key Laboratory of Land Surface Process and Climate Change in Cold and Arid Regions, Northwest Institute of Eco-Environment and Resources, Chinese Academy of Sciences, Lanzhou 730000, China

2 School of Atmospheric Sciences, Chengdu University of Information Technology, Chengdu 610225, China

3 CMA-NJU Joint Laboratory for Climate Prediction Studies, School of Atmospheric Sciences, Nanjing University, No. 163 Xianlin Avenue, Nanjing 210023, China

4 Department of Ecohydrology, Leibniz-Institute of Freshwater Ecology and Inland Fisheries, 12587 Berlin, Germany

temperature increase of even 1.5 °C will result in warming of ~ 2.1 °C in the TP region, in which case 36 ± 7% of the glaciers will disappear by the end of the century (Kraaijenbrink et al. 2017). The retreat rate of the glaciers is heterogeneous across the TP, being the smallest in the interior TP, and gradually increasing towards the margins along the Himalayas (Yang et al. 2019; Yao et al. 2019). Some of the glaciers in the Karakoram, Eastern Pamir, and Western Kunlun have even slightly advanced in recent years, the phenomenon termed the "Karakoram anomaly" (Brun et al. 2017; Farinotti et al. 2020; Forsythe et al. 2017; Lin et al. 2017). On one hand, the above regional trends were closely correlated with the precipitation variations, which decreased along the Himalayas while increased in the Inner TP and Pamir due to the weakened Indian Monsoon and strengthened westerlies (Gao et al. 2015; Yang et al. 2014; Yao et al. 2012b). On the other hand, the glaciers may respond differently to similar climatic variations, contributing to spatial variance in glacier mass balance (Fujita and Nuimura 2011; Sakai and Fujita 2017). In contrast to other regions of the TP, the glaciers and snowfall around the Karakoram are more sensitive to precipitation than to air temperature (Kapnick et al. 2014; Zhu et al. 2017). Moreover, the local differences in climatic factors and glacier topography, such as moisture recycling, seasonal precipitation distribution, orientation, and elevations, can lead to different mass balances even on the same glacier (Maussion et al. 2014; Yu et al. 2013).

As the "Water Tower of Asia", in addition to the glaciers, the TP is also covered by more than 1400 large (area > 1 km^2) lakes with a total area of $5.0 \times 10^4 \pm 791.4$ km^2, accounting for ~ 57.2% of China's lake area (Ma et al. 2010; Zhang et al. 2019b, c). The Inner TP is an endorheic basin containing most of these lakes in terms of number, area, and density (Zhang et al. 2020). Compared to the land surface, lakes are characterized by a larger heat capacity and a lower surface roughness, providing a persistent source of moisture to the lower atmosphere (Bonan 1995; Scott and Huff 1996). As a result, lake systems in regions with high lake density can significantly influence regional weather and climate (Notaro et al. 2013; Samuelsson et al. 2010; Thiery et al. 2015). This is also the case in the Inner TP, where lakes generally reduce regional temperature and increase local precipitation in summer (Wu et al. 2019b). Isolated from the influence of the Indian monsoon and westerlies, the Inner TP appears to be mainly controlled by the local water cycle, which can be significantly intensified by the abundant lakes in the region (Gao et al. 2020). In addition, individual lakes can also modify atmospheric circulation and thus precipitation distribution at the local level by inducing the lake breeze system, which is more pronounced when superimposed by that of the mountain-valley wind in areas with a complex topography (Gerken et al. 2013; Su et al. 2020).

The surface mass balance of glaciers, including mass gain by surface accumulation of snowfall and mass loss by ablation, is determined by the interaction between glacier surface, atmosphere, and snow cover (van Pelt et al. 2016). Rising air temperatures cause more surface melting, while the seasonal and perennial snow cover acts as a buffer against mass loss of glaciers beneath it (van Angelen et al. 2013). Based on the conclusions drawn from the studies mentioned above, it could be expected that the regional climate effects of the TP lakes, such as altering regional air temperature, humidity, and snowfall, may have a significant impact on glacier behavior. Research on this issue is still scarce: a recent study by de Kok et al. (2018) indicates that irrigation in the lowlands around TP may favor glacier growth in summer along the Kunlun Mountains and Pamir by increasing snowfall and decreasing net radiation. This study aims to explore the influence of the TP lakes on glacier behavior. For this purpose, we employ the air-lake coupled regional climate model to quantify the climatic effect of TP lakes and subsequently assess its potential impact on glacier behavior. Since glaciers in the Inner TP, especially those in Western Kunlun and Inner TP, mainly accumulate in spring and summer (Shen et al. 2022; Wang et al. 2017) and the climate effects of lakes are the strongest during the summer ice-free period (Wu et al. 2019b), we focused in the study on the summer period.

2 Data and methodology

2.1 Data

Given the scarcity of in-situ lake surface water temperature (LSWT) observations in the TP region, we employed the Global Observatory of Lake Responses to Environmental Changes (GloboLakes) data product v4.0 and the Moderate Resolution Imaging Spectroradiometer (MODIS) Land Surface Temperature (LST) version 6 products (MOD11C2/MYD11C2) to verify the simulated LSWT. The GloboLakes provides daily observations of LSWT for 1000 lakes globally for the period 1995–2016 at a spatial resolution of 0.05° Climate Modeling Grid (CMG), the temperatures from the different orbit instruments, including AVHRR (Advanced Very High Resolution Radiometer), AATSR (Advanced Along Track Scanning Radiometer) and ATSR-2 (Along Track Scanning Radiometer), were derived with the same algorithm and harmonized to ensure consistency (Politi et al. 2016), making GloboLakes perform well in comparison with in-situ measurements (Zhang et al. 2021). The MODIS products were composited and averaged from MOD11C1/MYD11C1 daily values to every eight days with a resolution of 0.05° CMG and an accuracy better than 2 °C over TP lakes (Song et al. 2016; Zhang et al. 2014).

ERA5 reanalysis 2 m air temperature product was also used in the evaluation of the WRF experiment in this study. ERA5 (Hersbach et al. 2020) is the newly released fifth-generation global reanalysis of the European Centre for Medium-Range Weather Forecasts (ECMWF). By combining model data with vast amounts of historical observations using advanced modeling and data assimilation systems, it provides hourly estimates of a large number of atmospheric, land and oceanic climate variables from 1950 to the present on a spatial resolution of about 25 km and resolves the atmosphere using 137 levels from the surface up to a height of 80 km. ERA5 can successfully capture the spatial distribution and the daily variation of 2 m air temperature over the TP with a slight cold bias when compared with in-situ observations (Ma et al. 2021, 2022).

The Tropical Rainfall Measuring Mission 3B42 Version 7 (TRMM-3B42V7) product was used to evaluate the simulated precipitation. The TRMM-3B42V7 dataset provides precipitation for the coverage of a global latitude band of 50° S–50° N with a spatial resolution of 0.25° and a temporal resolution of 3 h (Huffman et al. 2007). After bias adjustments using the Global Precipitation Climatology Center (GPCC) monthly gauge records, TRMM-3B42V7 has become quite a reliable precipitation dataset close to gauge observations in precipitation volumes over TP (Kanda et al. 2020; Kumar et al. 2021).

The MODIS daily snow cover products MOD10C1 Version 6 with a resolution of 0.05° CMG was used to validate the modeled snow. This dataset reports the percentage of snow-covered land computed when mapping the MOD10A1 cells at 500 m into a CMG cell at 0.05° resolution based on the Normalized Difference Snow Index (NDSI), which represents the state-of-the-art of global snow cover mapping algorithms (Da Ronco et al. 2020; Zhang et al. 2019d).

The National Centers for Environmental Prediction Global Final Analysis data (NCEP-FNL) with a 1° × 1° horizontal resolution and 6-h interval was used to form the initial and boundary condition for the Weather Research and Forecasting Model (WRF). The NCEP-FNL is derived from the Global Data Assimilation System (GDAS), which merges numerous data sources including remote sensing data assimilated together with surface and air reports from the global observation networks. The Global Lake Database version 2 (GLDBv2) with a horizontal resolution of 1 km developed by Choulga et al. (2014) and Kourzeneva et al. (2012) was used to obtain the lake locations and depths.

2.2 Model description and experimental designs

The Advanced Research WRF (Skamarock et al. 2008), a fully compressible and non-hydrostatic model, was used to carry out the simulations. The lake scheme in the WRF model, derived from the Community Land Model version 4.5 lake model, was implemented to predict lake thermal processes and consequently lake-atmosphere interactions. The lake model is a one-dimensional (1-D) mass and energy balance model that originated from the lake parameterization scheme of Hostetler et al. (1993) and was further modified and calibrated by Subin et al. (2012) and Gu et al. (2015). The model approximates a lake by 25 horizontal layers in total, including 10 lake water and ice layers, 10 soil layers of bottom sediment, and 5 snow layers above the lake ice, and solves the equation of vertical heat diffusion between each layer. The other selected physics parameterization options include the Yonsei University (Hong et al. 2006) planetary boundary layer scheme, the Noah land surface model (Chen and Dudhia 2001; Chen et al. 1996) with frozen soil and snow-cover prediction, the WRF Single-Moment 6-class (Hong and Lim 2006) microphysics scheme, the Grell-Devenyi ensemble (Grell and Devenyi 2002) cumulus scheme, the Dudhia (Dudhia 1989) shortwave radiation scheme, and the rapid radiative transfer model (Mlawer et al. 1997) for longwave radiation.

The simulation includes two two-way nested domains of 30 km and 10 km horizontal grid spacing in Domain 1 and Domain 2, respectively, with 31 vertical levels up to 50 hPa. The outer domain encompasses most of the Asia continent, the northern Indian Ocean, and part of the northwestern Pacific Ocean, allowing for incorporation of the influence of the summer monsoon on moisture transport and atmospheric circulation. The inner domain is centered over the south of the Inner TP and covers nearly the entire TP. Most of the lake grid cells are spread over the Inner TP, with altitudes ranging from 4000 to 5000 m a.s.l. (Fig. 1c), whereas ~ 57% of TP glacier area is located between 5000 and 6000 m a.s.l. (Guo et al. 2015). The initial and lateral boundary conditions were obtained from the NCEP-FNL data and updated every 6 h. The lake depth was obtained from the GLDBv2 dataset (Fig. 1b). The sea surface temperature was updated by the 0.5° × 0.5° daily real-time global sea surface temperature dataset (Thiebaux et al. 2003).

Based on the methods used in previous studies on the lake climate effects (Su et al. 2020; Wen et al. 2015; Wu et al. 2019b), we carried out two numerical experiments. The control (CTL) experiment uses the air-lake coupled WRF model for simulations with the lakes on the TP, while in the sensitive (SEN) experiment the lakes were replaced by a representative land use category of the surrounding land (mostly Grassland, Open Shrublands, and Barren or Sparsely Vegetated). The simulation period began on 20 May and ended on 31 August 2013. Only the model output results in summer (June, July, and August) were used after a 12-day model spin-up. The role of TP lakes in regional climate was revealed by the simulation differences between CTL and SEN experiments.

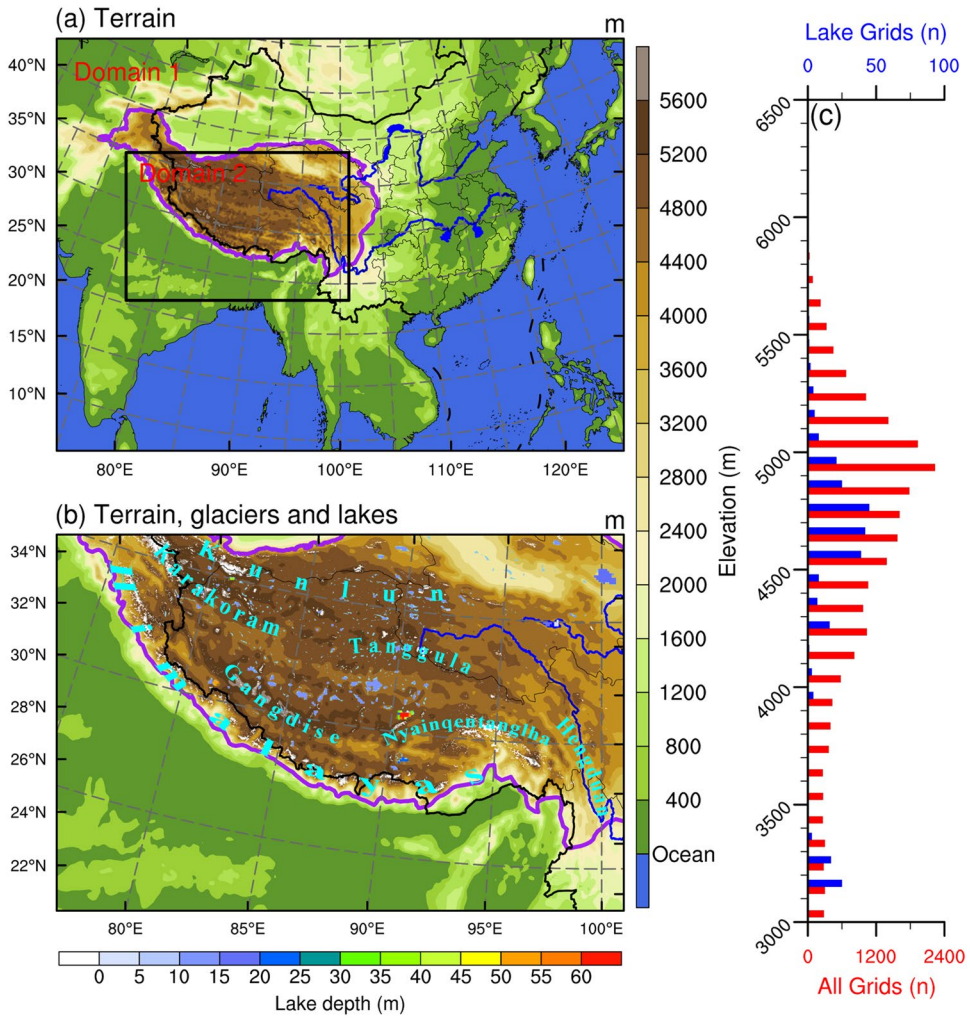

Fig. 1 **a** Geographic position and terrain height of the two nested domains applied in the WRF model. **b** Terrain height, lake distribution, and lake depth in Domain 2. **c** Numbers of total grid points (red bar) and lake grid points (blue bar) at different heights above 3000 m in Domain 2 (Note the different scales on the x-axes for total and lake grid points). In **a** and **b**, the purple line outlines the TP and the blue lines denote the Yangtze River and the Yellow River. The sky-blue area in **b** indicates the lakes while the white spots for glaciers and the cyan text mark the approximate location of the mountains

2.3 Methodology

Since the WRF model produces and represents snow at each grid in the form of snow depth (SD) and snow water equivalent (SWE), it needs to be converted to snow cover fraction (SCF) for validation against the MODIS snow cover product. The conversion relation varies significantly among different reanalysis data, ERA-Interim appears to perform the best in the TP (Orsolini et al. 2019). Hence, to convert the simulated SWE to SCF, we adopted the ERA-Interim equation (Loth and Graf 1998) as follows:

$$SCF = \min(1, SWE/15) \tag{1}$$

where SWE is the snow water equivalent (kg m^{-2}). A layer with an SWE of 15 kg m^{-2} represents 100% snow cover (15 cm depth assuming a constant snowfall density of 100 kg m^{-3}).

Atmospheric stability was indicated by the equivalent potential temperature (θ_e) as follows:

$$\theta_e = \left(T + \frac{L_v}{c_{pd}} r\right)\left(\frac{p_0}{p}\right)^{\frac{R_d}{c_{pd}}} \tag{2}$$

where T is air temperature (K) at the level of air pressure p, L_v is the latent heat of evaporation (2.5×106 J kg^{-1}), c_{pd} is the specific heat of dry air at constant pressure (1005.7 J kg^{-1} K^{-1}), r is the mixing ratio of water vapor (kg kg^{-1}), p_0 is the standard reference pressure (1000 hPa), p is the pressure at a given level, and R_d is the specific gas constant of air (287.04 J kg^{-1} K^{-1}).

3 Validation of WRF simulations

3.1 Lake surface water temperature

The incorporation of the lake module significantly improved the regional climate model's ability to simulate the thermal

characteristics of the lakes. To validate the modeled LSWT in terms of spatial distribution, we compared the LSWT simulated by CTL experiments with the GloboLakes observation data. As shown in Fig. 2, the WRF-Lake model accurately reproduces the surface water temperature of lakes in different regions across the TP with a mean bias of − 0.2 °C and RMSE of 3.2 °C in summer. For the Inner TP, where most of the lakes are concentrated, slight warm deviations exist in the lakes located over the south Inner TP, while cold bias appears in some small lakes located in the northeast and northwest of the Inner TP. The LSWT of several large lakes located in the northeastern part of the TP, including the largest brackish lake Qinghai Lake and the freshwater Lakes Ngoring and Gyaring, could also be well simulated by the model (Fig. 2c).

Additionally, the ability of the WRF-Lake model to reproduce the sub-seasonal variations of LSWT, 2 m air temperature, and air-lake temperature differences were also validated by comparison against the in situ observations of Li et al. (2016) over Qinghai Lake—the largest lake in the TP. Figure 3 demonstrates that the WRF-Lake model can reasonably represent the day-to-day evolution of these thermal characteristics in summer. The bias and RMSE between simulation and observation are − 0.56 °C and 0.89 °C for

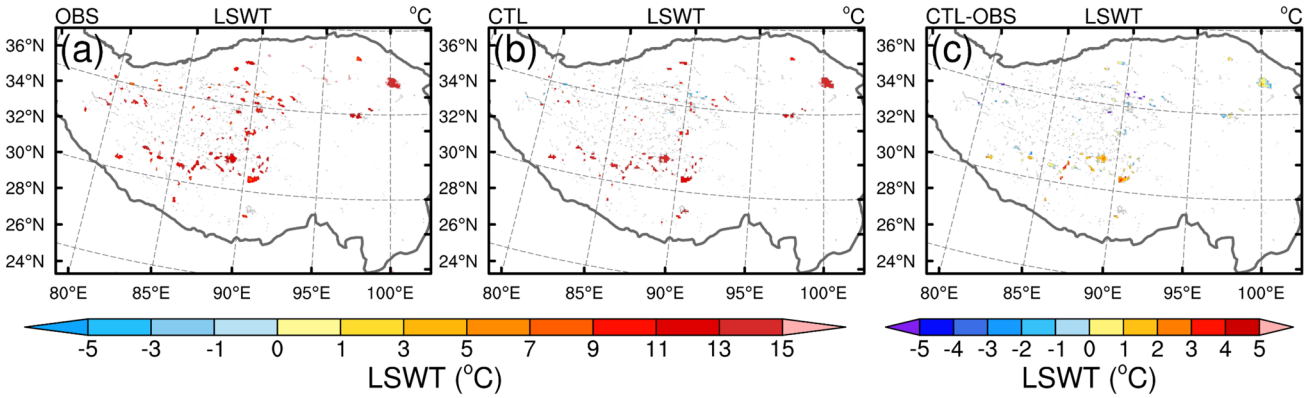

Fig. 2 The summer averaged lake surface water temperature from **a** GloboLakes observations, **b** CTL simulations, and **c** the differences between CTL simulations and observations over Domain 2

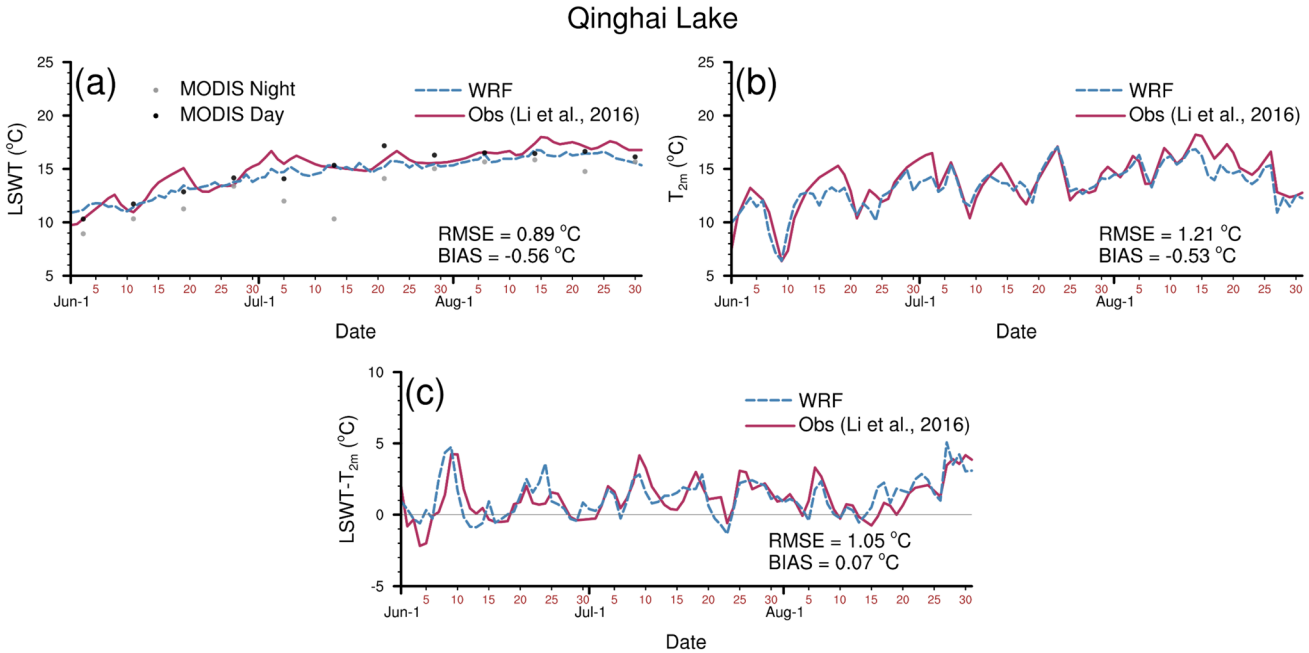

Fig. 3 The daily averaged **a** lake surface water temperature (LSWT), **b** 2 m air temperature, and **c** air-lake temperature differences between CTL simulations and observations by Li et al. (2016) over Qinghai Lake. The dots in **a** indicate MODIS observed lake surface temperature

LSWT (Fig. 3a), − 0.53 °C and 1.21 °C for 2 m air temperature (Fig. 3b), 0.07 °C and 1.05 °C for air-lake temperature difference, respectively (Fig. 3c).

The above comparison suggests that the WRF-Lake model is reliable in describing the lake thermal processes and consequently the air-lake interactions, essential for investigation of the role played by lakes in the climate-driven glacier dynamics over the TP region.

3.2 Air temperature, precipitation, and snow cover

The comparison with the ERA5 data shows that the WRF-Lake model can reasonably reproduce the spatial pattern of 2 m air temperature (T_{2m}), which gradually decreases with increasing altitude and is thus relatively low in the TP regions (Fig. 4a and b). Both observation interpolation method and model resolution limitations may lead to the unrealistic topography description, resulting in an apparent bias of T_{2m} in the regions with steep terrains. In our case, a slight cold bias in simulated T_{2m} generally appeared along the steep Himalayas and Hengduan Mountains, which might be attributed to the former reason, considering that most of the observations are concentrated in the lowland areas with higher T_{2m}. For other areas where the topography is not very steep, such as the Inner TP, the simulated T_{2m} is very close to the observations (Fig. 4c). While for most of the regions outside of the TP, the bias is less than 2 °C, except for southwest of the TP with a warm bias of about 2–6 °C.

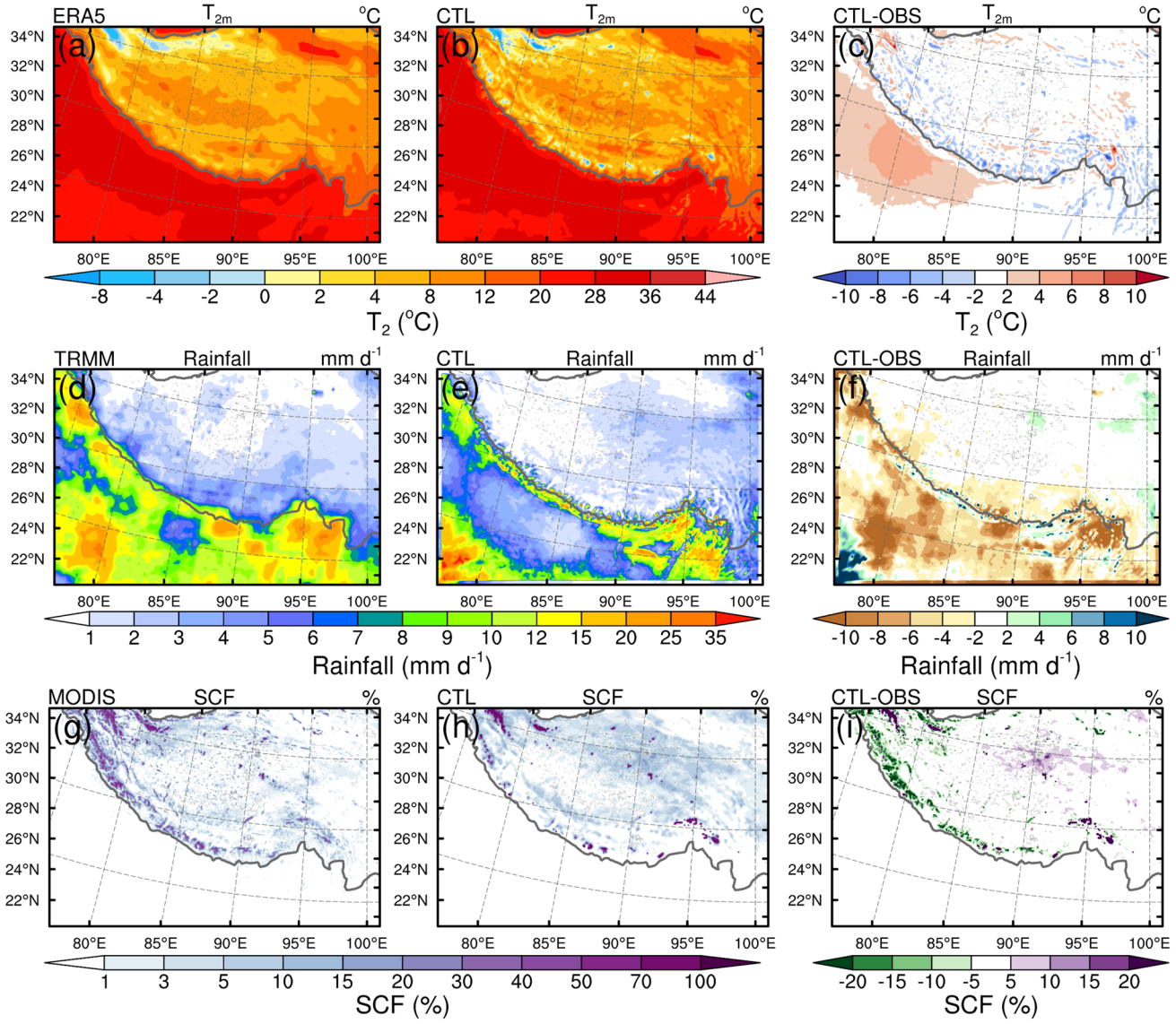

Fig. 4 The summer averaged **a**, **b** 2 m air temperature, **d**, **e** precipitation, and **g**, **h** snow cover fraction (SCF) from **a**, **d**, **g** observations, **b**, **e**, **h** CTL simulations, and **c**, **f**, **i** the differences between the CTL simulations and observations

Comparison with the TRMM observation shows that the WRF-Lake model also performs well in simulating the spatial pattern of precipitation, with less precipitation over the TP and more precipitation in the lower elevation region in the southwestern part of Domain 2 (Fig. 4d and e). However, there are still some discrepancies in the simulated magnitude of the rainfall distribution, especially along the steep Himalayas, which remains a long-lasting issue for many climate models (Yu et al. 2015). Although the model noticeably underestimates the precipitation along the Himalayas and its southwest regions, the bias is relatively smaller in the Inner TP regions (Fig. 4f).

The snow cover from MODIS observations exhibits notable spatial heterogeneity over the TP, correlating well with the spatial distribution of the highest mountains (Fig. 4g): the highest SCF was found in the northwestern, western, and southern edges of the TP, where the Kunlun, Karakoram, and Himalaya mountains are located. The SCF is also relatively higher in the southeastern part of the TP. Unlike the regions mentioned above, which have warm and moist air from the Indian Ocean and the Arabian Sea contributing to the higher SCF, the interior of the TP, shielded by the Himalayas and Karakoram mountains, has relatively low SCF despite an average elevation of about 5000 m. The snow cover pattern simulated by the WRF-Lake model is consistent with the perennial snow cover observed by MODIS, except that the model overestimates the SCF in the Karakoram and the Nyainqentanglha Mountains while underestimating it in the Himalaya mountains (Fig. 4i). However, the SCF in the Inner TP was relatively well simulated by the model.

To comprehensively evaluate the model performances, we give several statistics for summer mean T_{2m}, precipitation and SCF in Table 1, including pattern correlation, relative bias and root-mean-square-error (RMSE). The above evaluation results suggest that despite some regional biases along the steep Himalayas region, the WRF-Lake model can reasonably reproduce the T_{2m}, precipitation, and SCF over the Inner TP, appropriate for use in identifying the climatic effect of the TP lakes.

Table 1 The statistics between the simulations and observations for the 2 m air temperature, precipitation and snow cover fraction over Domain 2

Variables	Pattern correlation	Relative bias	RMSE
T_{2m}	0.99	2.67	2.06 °C
Precipitation	0.67	− 33.86	4.91 mm day^{-1}
SCF	0.63	− 7.84	6.55%

4 Potential impacts of TP lakes on glaciers

4.1 Lake effects on the 2 m air temperature and humidity

Figure 5 shows the differences in T_{2m} and Q_{2m} (2 m water vapor mixing ratio) between the simulation of two experiments with and without the TP lakes. As expected, the TP lakes noticeably decrease the summer surface air temperature and increase atmospheric humidity over the TP region, especially over the Inner TP, where the majority of lakes are concentrated: regionally averaged over the entire Inner TP, lakes decrease T_{2m} by − 0.17 °C (− 2.5%) and increase Q_{2m} by 0.15 g kg^{-1} (3.4%). These effects are more apparent over the lake surfaces, where the T_{2m} decreased by − 0.46 °C (− 4.6%), and Q_{2m} increased by 1.84 g kg^{-1} (34.1%) throughout the summer. In turn, the eastern and western parts of TP experience modest increase in temperature and decrease in humidity possibly due to the remote effect of Inner TP lakes by altering the atmospheric circulation. In the Himalayas, where glaciers are abundant but far away from the Inner TP lake cluster, lakes have limited effects on the air temperature and humidity. The variation in the region around the TP may be related to the changes in atmospheric circulation indirectly induced by the effects of the TP lakes. Since our study mainly focuses on the TP, the model results for the surrounding regions will not be discussed in detail.

4.2 Lake-induced changes in snowfall over glaciers

The differences in summer snowfall distribution between CTL and SEN experiments exhibit remarkable spatial heterogeneity (Fig. 6). For most of the western, southwestern, and southeastern parts of the TP and the northern Inner TP, where the Himalaya Mountains, Eastern Nyainqentanglha Range, and the central Kunlun Mountains are located, there show different reductions in snowfall, as cooling and moistening effects induced by the lake cluster through altering large-scale circulation are not evident or even opposite in these regions (Fig. 5). In contrast, most alpine areas of the eastern Inner TP, including the East Kunlun Mountains and the Tanggula Mountains, experienced more remarkable increases in summer snowfall due to the cooling and moistening effects of the TP lake cluster, as well as the low temperatures caused by higher altitude. Additionally, some localized but significant snowfall increase is concentrated over the southeastern and northwestern Inner TP, where the Western Nyainqentanglha Range and Western Kunlun Mountains are located. Despite several large lakes in the southern Inner

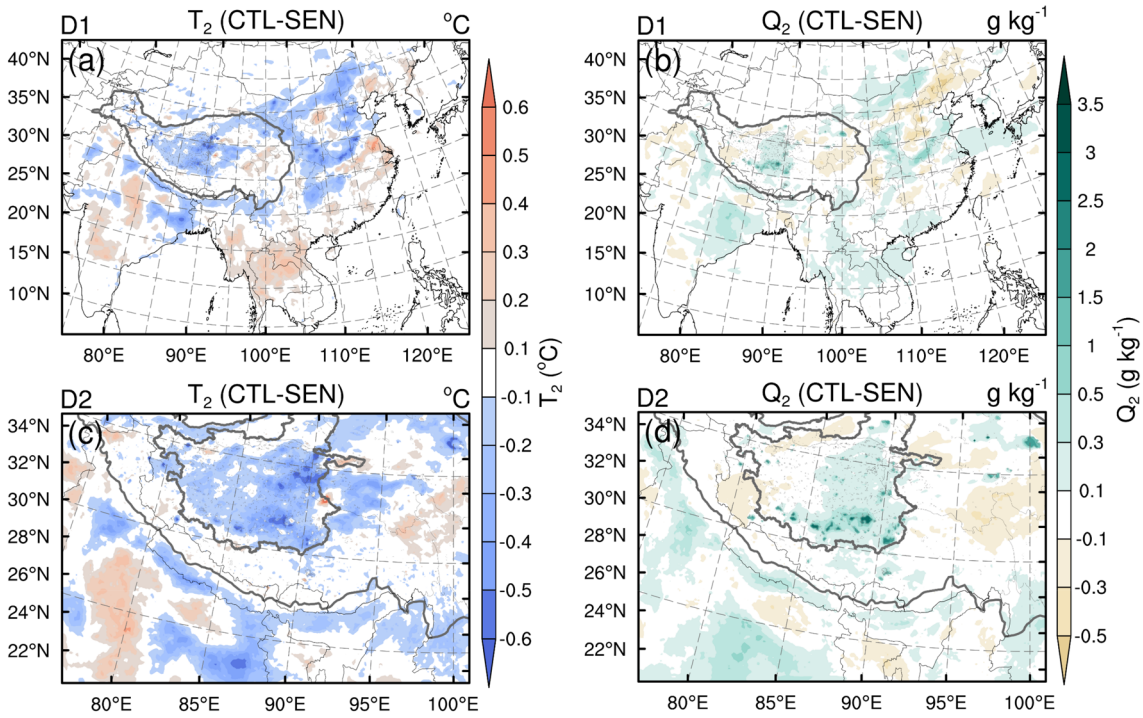

Fig. 5 The summer averaged differences of simulated **a**, **c** 2 m air temperature and **b**, **d** 2 m water vapor mixing ratio between CTL and SEN experiments in **a**, **b** Domain 1 and **c**, **d** Domain 2. The black line enclosing the area represents the Inner TP, where most TP lakes are concentrated

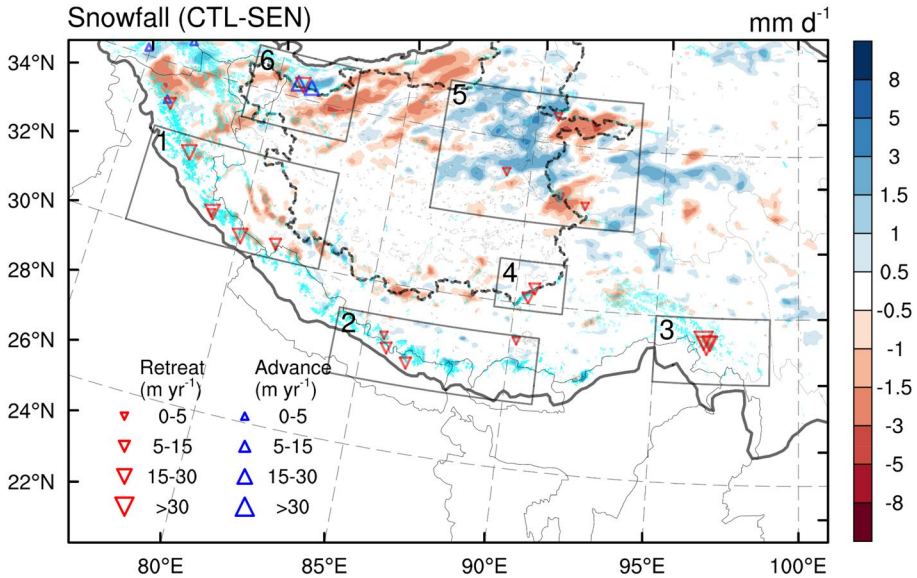

Fig. 6 The summer averaged differences in simulated snowfall between CTL and SEN experiments. The black dashed line enclosing the area represents the Inner TP. The cyan color indicates glaciers. The black boxes represent subregions 1–6. The red downward triangles indicate the retreating glaciers, and the blue upward triangles indicate the advancing glaciers. The observation data source is from Yao et al. (2012b)

TP exhibiting significant regional cooling and moistening effect (Fig. 5), almost no snowfall increase is identifiable around the lakes, only the Gangdise Mountains lying south of these lakes experiencing a snowfall variation primarily tend to reduce. The reason may be related to the terrain heterogeneity: the altitudes around these lakes are relatively lower compared to the Gangdise Mountains, corresponding to higher temperatures that lead to less snowfall and snowfall change in this region.

According to our simulations, the changes in snowfall caused by the TP lake cluster roughly coincide with the glacier changes obtained from both in situ observations (Yao et al. 2012b) and remote sensing data (Dehecq et al. 2019). To link the heterogeneous glacier, lake, and snowfall

patterns, we have divided the TP into 6 sub-regions with different trends in glacier mass balance and different lake abundances (Fig. 6):

- Subregions 1–3 are distributed along the Himalayas and are characterized by the strong glacier retreat and low amount of lakes: Subregion 1 (western Himalayas) with Glaciers Samudra Tapu, Dunagiri, Statopanth, Milam, and Naimona'nyi retreating at the rates of − 19.5 m yr^{-1}, − 3.0 m yr^{-1}, − 26.9 m yr^{-1}, − 26.6 m yr^{-1}, and − 5.0 m yr^{-1} respectively. Subregion 2 (central Himalayas) includes Dasuopu (− 4.1 m yr^{-1}), Middle Rongbu (− 8.8 m yr^{-1}), AX010 (− 6.9 m yr^{-1}), and Qiangyong (− 2.4 m yr^{-1}) Glaciers. Subregion 3 is the southwestern TP characterized by the most pronounced glacier retreat (Ata Glacier − 56.1 m yr^{-1}, Parlung No.4 − 15.6 m yr^{-1}, and Yanong − 73.0 m yr^{-1}).
- The Inner TP (Subregions 4, 5 and 6) has generally lower rates of glacier retreat: Subregion 4 (the Western Nyainqentanglha Range) contains large Nam Co and is exemplified by Glaciers Zhadang (− 10.8 m yr^{-1}) and Gurenhekou (− 8.1 m yr^{-1}). Subregion 5 in the eastern Inner TP is covered by numerous small lakes and has glacier typical retreat rates of − 3.4 m yr^{-1}, − 1.0 m yr^{-1}, and − 1.7 m yr^{-1} for Glaciers Xiaodongkemadi, Malan and Purogangri, respectively. Subregion 6 (the Western Kunlun Mountains), where a few small lakes are located, has the lowest rates of glacier contraction, including Glaciers Kunlun (+ 27.3 m yr^{-1}), Yulong (+ 16.3 m yr^{-1}), and Duofeng (− 27.6 m yr^{-1}).

As it is seen from the values above and mentioned in the Introduction, the glaciers in the Inner TP, which are less influenced by the atmospheric circulation systems than the glacial regions of the Himalayas and eastern Pamir, are dominated more by continental climatic conditions determining a higher local precipitation recycling ratio in this region (Gao et al. 2020). Herewith, the lake evaporation may play an essential role in enhancing regional snowfall and decelerating thereby the local glacier retreat. Therefore, to comprehensively analyze the lake effects on glacier behavior, we concentrate the detailed analysis on Subregions 4–6 belonging to the Inner TP, as containing the major glaciers of the Inner TP and experiencing the most pronounced lake effects according to model simulations.

4.3 Regional-scale interactions over the inner TP

4.3.1 Western Nyainqentanglha Range (Subregion 4): effects of a large lake on moderate glacier retreat

The Western Nyainqentanglha Range is located in the southeastern Inner TP. Glaciers in this region are influenced by both the continental climate and the Indian Summer Monsoon. Adjacent to its northern slope is Nam Co, which is currently the second-largest (before 2001, the largest) endorheic lake in the Inner TP, significantly affecting the local climate. According to the modeling outcomes, the lake cooling effect and the intense evaporation in summer resulted in a substantial air temperature drop and humidity increase in this region (Fig. 7a and b). As a result, both snowfall on the Western Nyainqentanglha Range and snow depth on the surface of the glaciers increased (Fig. 7c and d), indicating that the presence of Nam Co may facilitate preservation of glaciers on the Western Nyainqentanglha Range in summer.

Figure 8 illustrates the role of Nam Co in the local glacier behavior by presenting a meridional transect crossing the lake and glaciers over the Western Nyainqentanglha Range from north to south (see the red line in Fig. 7). Taking into account the diurnal variations of the lake-induced circulation (Su et al. 2020; Wu et al. 2019b), we considered the lake effect during daytime and nighttime separately.

During daytime, Nam Co is a source of cooling and moisture (Fig. 8b and e). Based on Eq. (2), the humidity increase can increase θ_e and destabilize thereby the atmospheric boundary layer. However, the cooling effect leads to strong downdraft and suppresses instability over the lake: The enhancement in humidity and θ_e is confined to the lake area, while both moisture and θ_e decrease significantly with the height, which effects extend up to 8 km upwards and cover the entire north slope of the Western Nyainqentanglha Range (Fig. 8h). The subsidence over the lake stabilizes the atmospheric boundary layer and decreases precipitation over the lake area and its adjacent land (including the north slope of the Western Nyainqentanglha Range). Additionally, the divergent surface flow formed a lake breeze transporting low-level moisture uphill along the north slope and then to the other side of the mountain, where it converged with the Indian summer monsoon from the south and further led to the increase of precipitation on the southern slope. The temperature near the peak of the mountain is below 2.5 °C, causing precipitation in snow form (Deng et al. 2017; Ding et al. 2014) and diminishing thereby glacier ablation.

During nighttime, Nam Co warms and moistens the atmosphere over the lake area (Fig. 8c and f). The lake-induced updraft transports the evaporated moisture from the lake upwards, to increase θ_e and destabilize the atmosphere over the lake and surrounding land (Fig. 8i). From Fig. 8c, when the Indian monsoon climbs over the mountain, part of the airflow is heated by condensation and thus ascends, while the rest turns to a downhill wind along the north slope to the lake. Nam Co reinforces this process by generating updrafts over the lake that induced compensatory strengthening of the downhill wind, leading to precipitation increase over the southern slope. The downhill wind further warmed and moistened by the

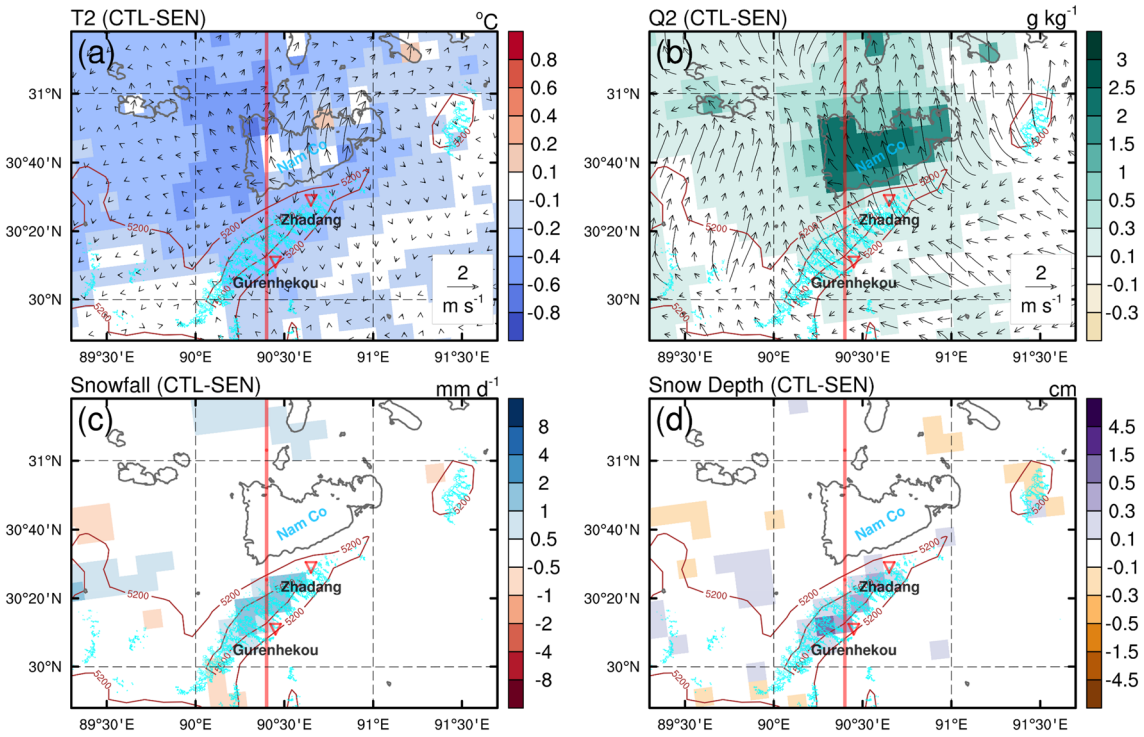

Fig. 7 The summer mean differences of simulated **a** T_{2m}, **b** Q_{2m}, **c** snowfall, and **d** snow depth between CTL and SEN experiments over Subregion 4. The streamline in **a** and **b** represents the 10 m wind of the CTL-SEN and CTL experiment, respectively. The cyan curve outlined the glaciers. The brown curve outlined the terrain height (only altitudes above 5200 were shown). The triangles for single glaciers correspond to the meaning of Fig. 6. The red line represents the transection used for the vertical cross-section

lake, getting unstable and turning into updrafts, resulting in precipitation increase over the north slope. Hence, during nighttime, Nam Co increases precipitation over both the north and south slopes of the Western Nyainqentanglha Range. Usually, the maximum snowfall is expected at the surface air temperatures between 1 and 2 °C (Deng et al. 2017), and the snowline ranges from 4700 to 5100 in summer (Pu and Xu 2009). Considering that nighttime temperatures in the upper mountain areas stay below 2.5 °C (Ding et al. 2014), the increased precipitation should result in snow cover increase beneficial for glacier preservation.

Overall, Nam Co lowers the air temperature and increases snow cover over the Western Nyainqentanglha Range, potentially preventing the glacier from ablating. The simulation results also indicate that the lake effect, combined with the Indian Summer Monsoon and the topography effects around the lake, produces more snow cover on the southern slope of the mountain, contributing thereby to higher glacier coverage and slower retreat rate compared with the northern slope, which has confirmed by many observational studies (Bolch et al. 2010; Wu et al. 2016; Yu et al. 2013; Zhang and Zhang 2017).

4.3.2 Eastern Inner TP (Subregion 5): numerous small lakes slowing down glacier retreat

The eastern Inner TP hosts numerous small lakes, and several major glaciers, enabling a comprehensive investigation of the TP lake cluster effect on the glacier behavior. As shown in Fig. 9a, the TP lake cluster significantly reduces the T_{2m} in summer over most of the eastern Inner TP. This cooling effect is generated by many individual small lakes, triggering divergent flows over them, and eventually extending throughout the region. The only exception is the increased T_{2m} with the convergent surface flow over the east Tanggula Mountains. Every lake in the eastern Inner TP appears to be a moisture source increasing significantly Q_{2m} over the lake and in its vicinity, with a spreading area in the downwind direction (Fig. 9b). In addition to temperature, humidity, and circulation variations, the snowfall increases in most alpine parts of this subregion, except east Tanggula Mountain and the northeastern part (Fig. 9c). Lake-induced changes in snow depth distribution are essentially the same as those of snowfall, but more concentrated in alpine areas.

To further reveal the mechanism of lake climate effect on glacier behavior, we traced the model output along the

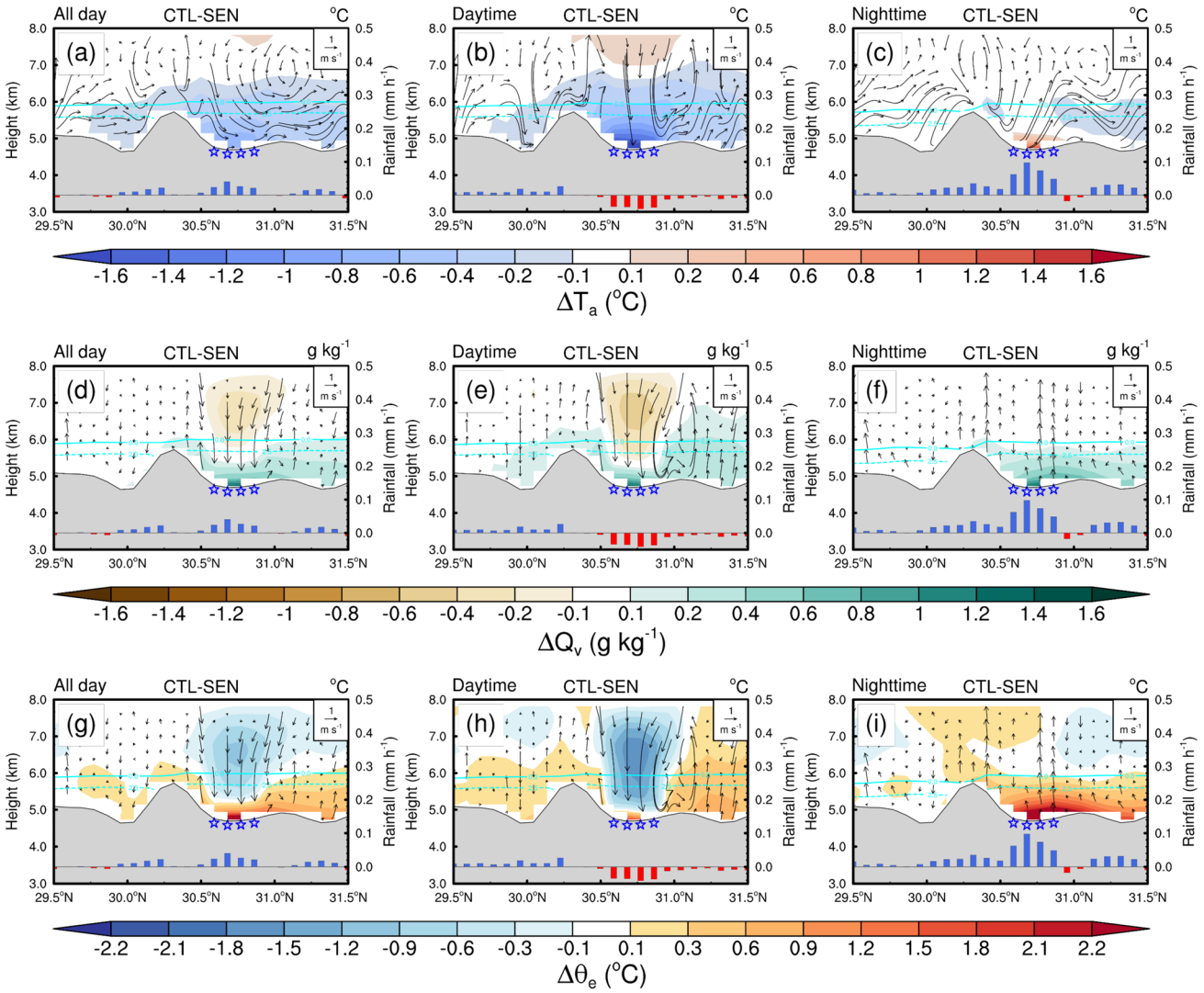

Fig. 8 The height-latitude cross-sections along the red line in Fig. 7 of the simulated mean differences in **a–c** air temperature, **d–f** water vapor mixing ratio, and **g–i** equivalent potential temperature between the two experiments (CTL-SEN). Vertical circulation (vectors) in **a–c** from CTL experiments, while others were differences between the two experiments (CTL-SEN); the vertical velocity was magnified by 100 times. The bar indicates precipitation differences (CTL-SEN) at corresponding locations. The blue star represents the grids of Nam Co Lake. The solid and dashed cyan lines represent 0° and 2.5° isotherms, respectively

meridional transection starting at Purogangri Glacier, passing through Chibuzhang Co (33.4819° N, 90.3625° E) and Tanggula Mountain, and ending behind Xiaodongkemadi Glacier (solid red line in Fig. 9). As above, the daytime and nighttime patterns were considered separately.

During daytime, lakes chill and humidify the atmosphere in boundary layer, especially over the lake surface (Fig. 10b and e). Similar to the effects of Nam Co, the instability of the atmospheric boundary layer over Chibuzhang Co caused by the moisture increase is suppressed by the strong daytime cooling effect of the lake, which induced downdrafts over the lake (Fig. 10h). The subsidence and divergent flow over the lake formed a lake breeze that advected moisture uphill along the slope of the west Tanggula Mountain. Cooling of the moist air from the lake during uplift along the windward slopes promotes condensation and precipitation, leading to moisture detachment and irreversible latent heating, possibly contributing to the lee side warming (Elvidge and Renfrew 2016).

During nighttime, the cooling effect of the TP lakes weakens while their humidifying effect enhances (Fig. 10c and f). Chibuzhang Co leads to instability of the overlying atmosphere and generated updrafts incline toward Tangula Mountain directed by the background winds, which increases the precipitation over the lake and the west slope of Tanggula Mountain (Fig. 10i). In turn, the development of downdraft branches over the peak and the east of

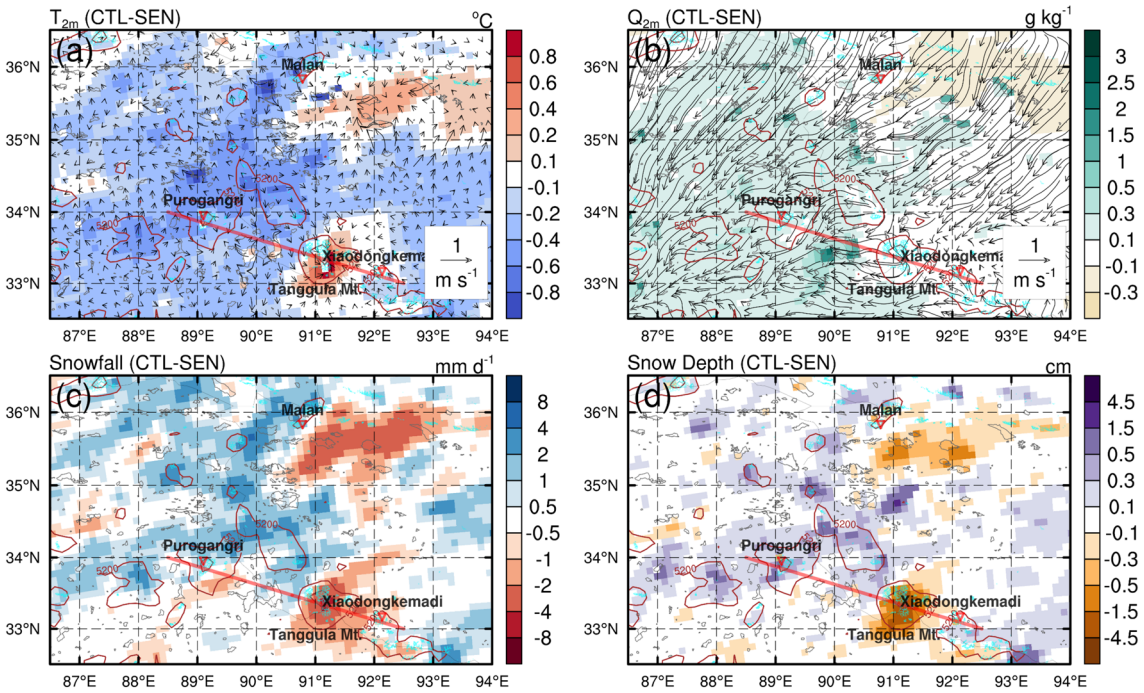

Fig. 9 The summer mean differences in the simulated **a** T_{2m}, **b** Q_{2m}, **c** snowfall, and **d** snow depth between CTL and SEN experiments over subregion 5. The streamline in **a** and **b** represents the 10 m wind of the CTL-SEN and CTL experiment, respectively. The cyan curve outlined the glaciers. The brown curve outlined the terrain height (only altitudes above 5200 m were shown). The triangles for single glaciers correspond to the meaning of Fig. 6. The red line represents the transection used for the vertical cross-section

Tanggula Mountain suppresses the convective precipitation and warms the atmosphere through the dry adiabatic process.

In summary, the TP lake cluster potentially preserves the glaciers in the eastern Inner TP region by cooling and moistening the atmosphere and increasing snowfall. The presence of Chibuzhang Co modifies the local circulation and precipitation distribution, favoring the preservation of glaciers on the western slope of Tanggula Mountain while having the opposite effect on the glaciers on the other side. It may be one of the reasons for the observed faster glaciers retreat on the east slope than those in the west (Duan et al. 2019).

4.3.3 Western Kunlun Mountains (Subregion 6): large-scale lake effect, slowest glacier retreat

Compared to the Eastern Inner TP, lakes located in this region are both less abundant and smaller in size, resulting in relatively weak lake-induced local cooling and moistening to the low lever atmosphere (Fig. 11a and b). Nevertheless, lakes induce here drastic changes in the spatial pattern of snowfall and snow depth, both increasing on the north side of the Western Kunlun Mountains and its peak while decreasing on the mountain's south slope. One explanation for such a noticeable snowfall increase may be ascribed to the lower air temperatures in the Western Kunlun, whose most part is below 0 °C (not shown). It increases the probability of snow precipitation and preserves snow and glaciers by reducing their sensitivity to warming (Sakai and Fujita 2017; Zhu et al. 2017). The different accumulation regimes for the north (summer accumulation type) and south slopes (winter accumulation type) of the western Kunlun Mountains (Maussion et al. 2014; Molg et al. 2014) may lead to increased snowfall along the north slope.

Considering the local lakes have limited effects on climate in this region, an alternate reason for such a snowfall pattern may be related to the lake-induced atmospheric circulation changes. These involved circulation systems including the South Asian high and westerlies, which are represented by geopotential height and wind at 200 hPa in the CTL experiment (Fig. 12a). The CTL-SEN experiments demonstrated that the TP lakes reduce the 200 hPa geopotential height over the north TP and increase it over the south TP, reinforcing the South Asian high and thus southwardly strengthening the westerlies above the Western Kunlun Mountains (Fig. 12b). In such a case, the precipitation increase, and air temperature decreases in the Western Kunlun Mountains according to a previous study by Molg et al. (2014). Meantime, the CTL experiment shows that the TP has a low geopotential height at 500 hPa level, which forms a cyclonic circulation that in synergy with the Asian monsoon can transport water vapor from the TP, Indian Ocean, and Bay of Bengal to the north

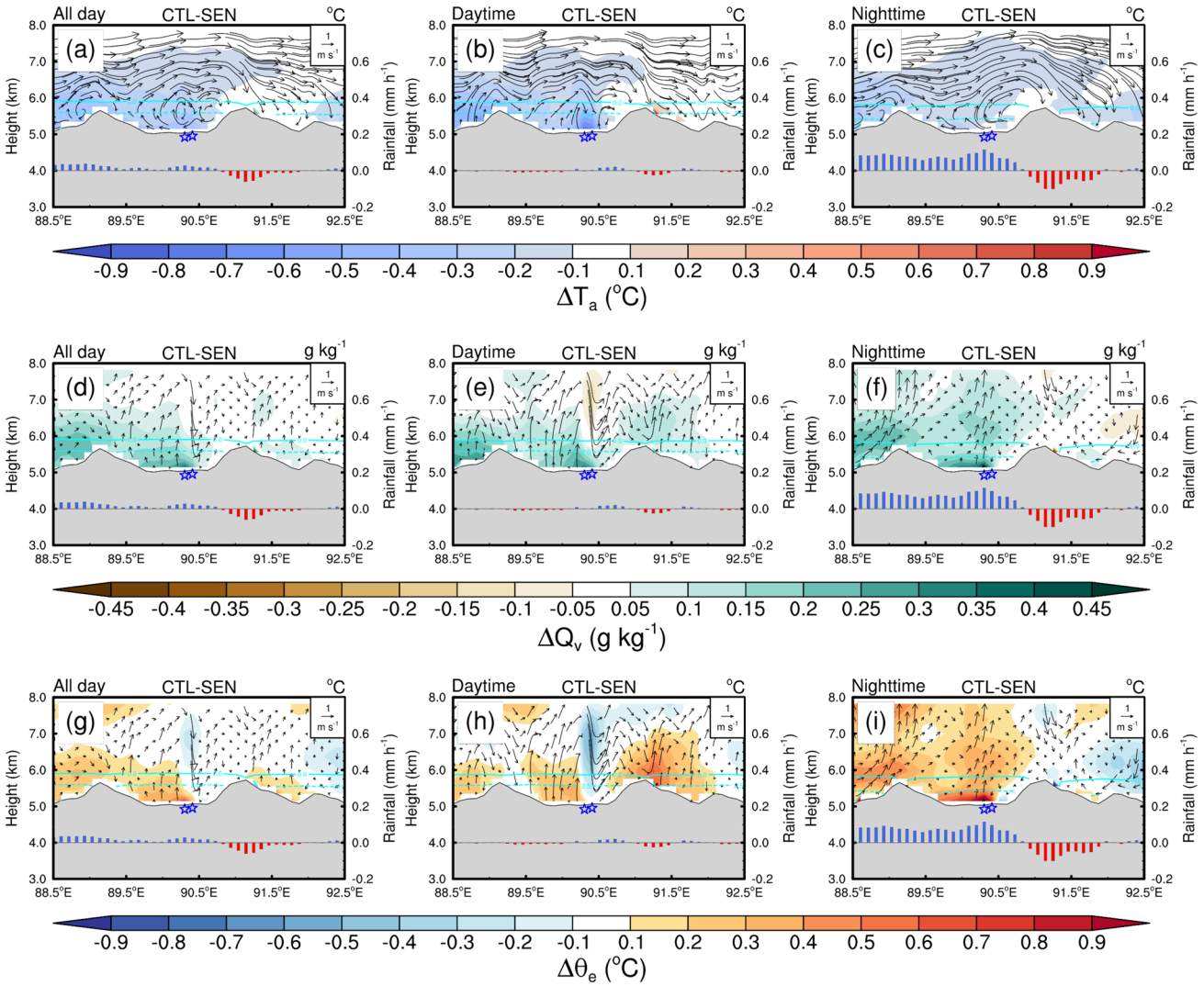

Fig. 10 The height-longitude cross-sections along the red line in Fig. 9 of the simulated mean differences in **a–c** air temperature, **d–f** water vapor mixing ratio, and **g–i** equivalent potential temperature between the two experiments (CTL-SEN). Vertical circulation (vectors) in **a–c** from CTL experiments, while others were differences between the two experiments (CTL-SEN); the vertical velocity was magnified by 100 times. The bar indicates precipitation differences (CTL-SEN) at corresponding locations. The blue star represents the grids of Chibuzhang Co. The solid and dashed cyan lines represent 0° and 2.5° isotherms, respectively

TP (Fig. 12c) (Zhang et al. 2019a). The TP lakes reinforce this effect by lowering the 500 hPa geopotential height over TP and providing the water vapor through evaporation, contributing to the snowfall increase in the Western Kunlun Mountains (Fig. 12d).

5 Discussion

5.1 Regional differences in the impacts of lakes on glaciers

According to our study, the TP lake cluster can influence the behavior of glaciers at various spatial scales. In contrast to the glaciers along the Himalayas (Subregions 1, 2 and 3), which are weakly affected by the TP lakes and not discussed in detail here, the glaciers in Inner TP (Subregions 4, 5 and 6) reflect different lake-induced impacts.

The local lake effect is most apparent in the glaciers on the Western Nyainqentanglha Range (Subregion 4). Nam Co with an area of 2012 km^2 (in 2018), which is three times the size of glaciers adjacent south of it (Luo et al. 2020; Zhang et al. 2019b), exerts an apparent influence on the glaciers by regulating local air temperature, moisture, and circulation. This influence superimposes that of the Indian monsoon, increasing the snowfall over the entire mountain range, especially on the southern slope. The average retreat rate for glaciers in this region is − 9.45 m yr^{-1}, much slower than that

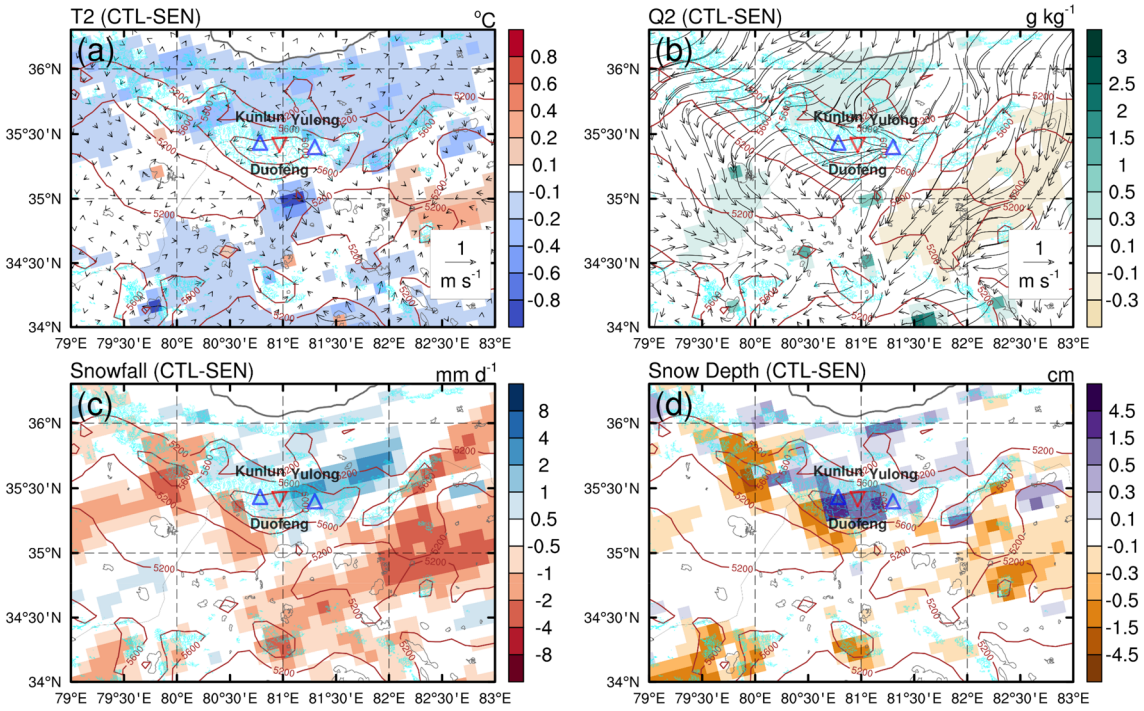

Fig. 11 The summer mean differences of simulated **a** T_{2m}, **b** Q_{2m}, **c** snowfall, and **d** snow depth between CTL and SEN experiments over subregion 6. The streamline in **a** and **b** represents the 10 m wind of the CTL-SEN and CTL experiment, respectively. The cyan curve outlined the glaciers. The brown curve outlined the terrain height (only showing altitudes above 5200). The triangles for single glaciers correspond to the meaning of Fig. 6

of the glaciers along the Himalayas (subregions 1–3), which retreat at an average rate of − 20.66 m yr^{-1}. And the Zhadang Glacier on the north slope retreated faster (− 10.8 m yr^{-1}) than Gurenhekou Glacier (− 8.1 m yr^{-1}) on the south slope (from the 1970s to 2000s), which was also confirmed by many other observational studies (Bolch et al. 2010; Wu et al. 2016; Yu et al. 2013; Zhang and Zhang 2017). For the Eastern Inner TP (Subregion 5), the lakes affect glaciers on both regional and local scales. Here, the cumulative effect of TP lakes as a cluster reveals itself in generally lower air temperatures and increased snowfall on a regional scale, contributing to the preservation of the glaciers. Compared to Subregion 4, the lake climate effects generated by numerous small lakes in Subregion 5 are much stronger. Accordingly, the average rate of glacier retreat in Subregion 5 is also much slower, with a rate of − 2.03 m yr^{-1} compared to − 9.45 m yr^{-1} in Subregion 4 (Yao et al. 2012b). In turn, the relatively large Chibuzhang Co affects the Tanggula Mountains glaciers to the east of it by altering local circulation and the snowfall distribution, favoring the preservation of glaciers on the western slope at the cost of accelerated glacier retreat on the east slope. Hence, Nam Co (Subregion 4), which is larger and closer to the glacier compared to Chibuzhang Co (Subregion 5) produces a completely different effect on the glaciers. Herewith, our results suggest different or even opposite impacts of lakes on glaciers depending on the lake size and the distance between the lake and glaciers. Our results also confirm that the location of the glaciers on the windward or leeward of the mountain plays an essential role in the response of glaciers to the lake effect (Maussion et al. 2014). The Western Kunlun Mountains is one of the few regions in the TP revealing balanced to slightly positive glacier mass budget in recent years, especially since 2010 at its north slope (Cao et al. 2020; Hewitt 2005). In contrast to the Western Nyainqentanglha Range (Subregion 4), the lakes near the Western Kunlun Mountains (Subregion 6) are much smaller than the glaciers in this region, leading to a weak local impact on glaciers. Hence, the lake-induced significant increase in snowfall over the Western Kunlun Mountains may be tentatively ascribed to the accumulated large-scale effect of the TP lake system.

5.2 Relation of lakes to other factors affecting glacier changes

Our results demonstrate that lakes of the TP can accelerate (or dampen) global climate effects on the glacier mass balance. In the Western Nyainqentanglha Range (Subregion 4), the precipitation decreases slightly in 1970–2007 due to weakening Indian monsoon and strengthened westerlies,

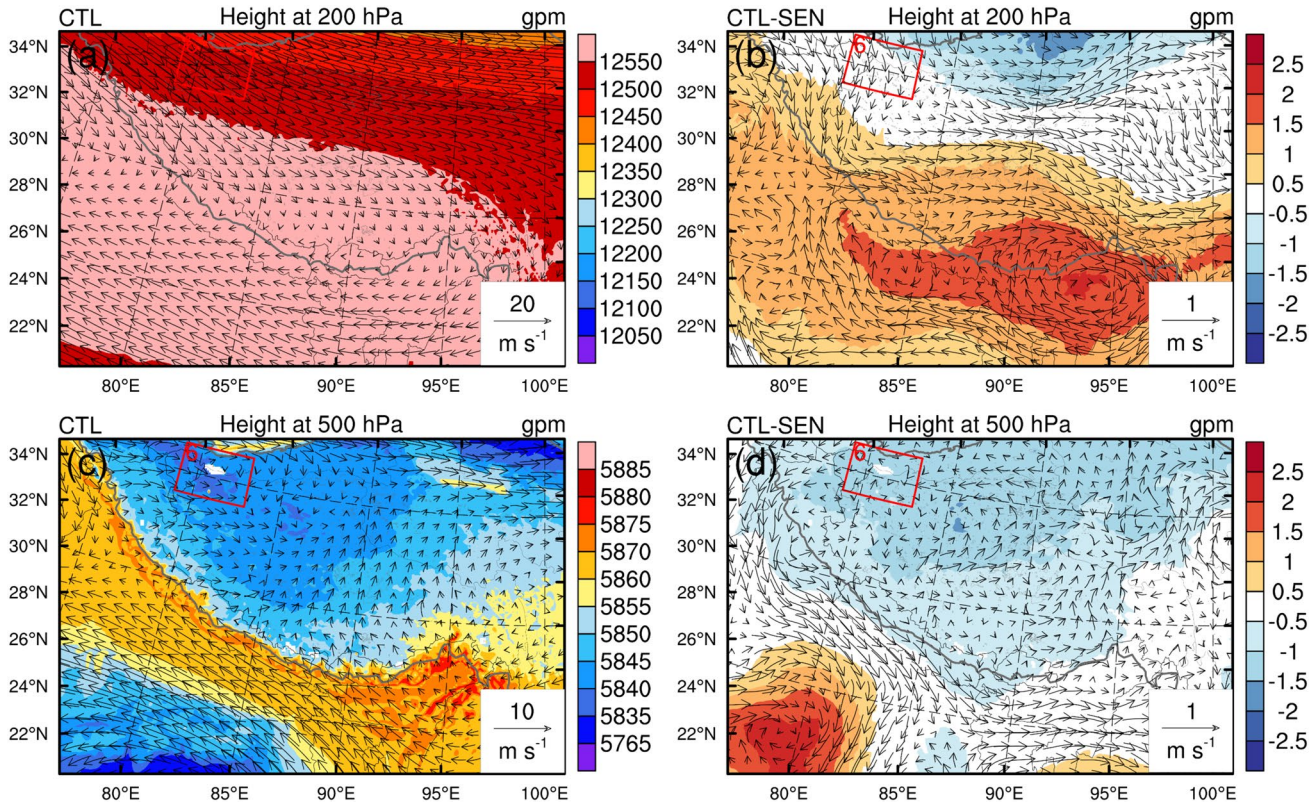

Fig. 12 The geopotential height (gpm) and corresponding wind from (left column) CTL and (right column) CTL-SEN experiments at **a**, **b** 200 hPa and **c**, **d** 500 hPa, respectively. The red box indicates the location of subregion 6

with the trend growing from the south (− 0.26 mm yr^{-1}) to the north (− 1.5 mm yr^{-1}); the air temperature rise was also more apparent at the north slope (0.043 °C yr^{-1}) compared to the south one (0.036 °C yr^{-1}), resulting in a more intense retreat of glaciers in the north slope (Yu et al. 2013). Our results have shown that Nam Co can form a local lake-land breeze system superimposed with mountain-valley winds, which interacts with the Indian Moonsoon by intensifying snowfall at the southern slope and further strengthening the climate effect on the glaciers.

In the eastern Inner TP region (Subregion 5), the warming rate in the Tanggula Mountains during 1969–2015 was reported as 0.038 °C yr^{-1}, while annual precipitation slightly increased by 0.4% (Duan et al. 2019). The glaciers in this area are more sensitive to summer air temperatures than to precipitation (Zhang et al. 2018). Here, both Xiaodongkemadi Glacier, Glaciers in Geladandong Peak of Tangula mountains, and Purogangri Glacier are located in the eastern Inner TP, implying generally similar climatic conditions, glacier type, and their lack of debris cover. However, the retreat rates of these three glaciers are quite different. Xiaodongkemadi Glacier experienced the greatest mass loss due to its smallest area, followed by Glaciers in Geladandong Peak, while Purogangri Glacier experienced the least mass loss, although its size is only half of the former one (Zhang et al. 2018). Our results correspond well to the above discrepancy of glacier dynamics, demonstrating that lakes decrease T_{2m} (about − 0.4 to − 0.6 °C) and increase snow depth (about 0.5–1.5 cm) at Purogangri Glacier, while increase T_{2m} and reduce snow depth at Geladandong Peak.

In recent years, glaciers in the Western Kunlun Mountains (Subregion 6) experienced trends in contrast to those in other regions of the TP (Cao et al. 2020). Generally, decreased air temperatures and increased precipitation in summer were assumed to be the reasons for positive glacier mass balances in this region (Cao et al. 2020; Fowler and Archer 2006; Sakai and Fujita 2017). However, the drivers of the observed temperature and precipitation changes remain uncertain. Compared to the Western Nyainqentanglha Range, which is strongly affected by the Indian monsoon, Western Kunlun's climate is dominated by the westerlies and the Tibetan anticyclone (Farinotti et al. 2020). The strengthened westerlies would cause increased precipitation and decreased air temperature in Western Kunlun (Molg et al. 2014), favoring the growth of glaciers in this region, which is less sensitive to climate warming (Zhu et al. 2017). These variabilities may be related to the "Western Tibetan (Karakoram) Vortex", an anomalous deep vortex circulation system above

the Karakoram in the western TP, through its interaction with the south Asian monsoon (Forsythe et al. 2017; Li et al. 2018b; Zhao et al. 2014). In the case of "Karakoram Anomaly", for instance, an anomalous southward intensification of the westerlies can result in a negative phase of "Western Tibetan (Karakoram) Vortex" with cyclonic circulation over the central Karakoram, which corresponds to the upward vertical circulation anomalies that lead to an anomalous volume expansion and yields adiabatic cooling of the air from surface-level to tropopause, especially in a weakening south Asian monsoon conditions. As a region with the most vital land–atmosphere interactions in the mid-latitude areas, the TP surface processes play an essential role in regional climate (Wu 2020), while snow cover over the TP act as an elevated cooling source due to its albedo and thermodynamic effect, can reduce the upper-level geopotential height and modulate the atmospheric circulation (Li et al. 2018a). Our results are in line with the above findings, suggesting that the TP lakes can reduce the 200 hPa geopotential height and form a cyclonic circulation above the northern TP by increasing the snowfall in the Inner TP, strengthening the westerlies southward in the Karakorum. Correspondingly, the increased precipitation and decreased air temperature facilitate glacier preservation or even growth in the Western Kunlun Mountains.

However, it should be noted that although TP lakes can slow the retreat rate of glaciers in Inner TP, it is unlikely to stop the trend under the global warming background. According to a recent study, the "Karakoram anomaly" comes to an end after 2015, but the thinning rate of glaciers is still the slowest over the Karakoram and Kunlun Mountains compared to other places in the TP (Hugonnet et al. 2021). This implies that climate change remains the dominant influence relative to the effect of the TP lakes on glacier behavior.

6 Conclusions

We applied the air-lake coupled WRF-Lake model at a high spatial resolution to simulate the climate effect of the TP lake cluster and to evaluate the potential lake impacts on glacier retreat. Experiments with and without the TP lakes were conducted in the summer of 2013 to quantify the climate effects of the TP lakes at local to regional scales.

Initially, the capability of the model in simulating LSWT, T_{2m}, precipitation, and snow cover in summer was evaluated by comparing with observations. The results indicate that the model can reasonably reproduce the spatial distribution of LSWT for all TP lakes during summer, with a bias of − 0.2 °C and RMSE of 3.2 °C, as well as the daily variation of LSWT in Qinghai Lake, with a bias of − 0.56 °C and RMSE of 0.89 °C. The model also performed well in simulating the spatial pattern of T_{2m}, precipitation, and snow cover over the TP.

According to our results, the TP lakes potentially affect the glacier behavior by altering regional climate, especially over the Inner TP, where the majority of the TP lakes are concentrated. Generally, the lakes tend to reduce the air temperature and increase air humidity, with variations of − 0.17 °C (− 2.5%) and 0.15 g kg^{-1} (3.4%) averaged over the entire Inner TP, respectively. As a result, the snowfall distribution can also be changed with apparent spatial heterogeneity due to the effects of the TP lakes. Snowfall is reduced by the TP lakes over the Himalaya Mountains, the Gangdise Mountains, the southeastern TP, and the central Kunlun Mountains due to the weak or counteracting lake effects on temperature and humidity in these regions. In contrast, the snowfall in Inner TP is increased due to the dominant cooling and humidifying effects of the TP lakes. The observed glacier retreat in past decades is negatively correlated with the simulated lake-induced snowfall changes: the most intensive glacier retreat occurred along the Himalayas, especially in the southeastern TP, and generally decreases from the Himalayas towards the Inner TP. Our results demonstrate that the lake-induced air temperature decrease and the snowfall increase make a contribution to the glacier response to climate warming and changing atmospheric circulation patterns. Limitations of this modeling study include inevitably rough representation of lake morphometrical and physical characteristics, as well as ignoring of a large number of small sub-grid scale lakes, which increases uncertainty in modeling of the regional-scale lake effects. Improving the lake parameterization as well as the model resolution in the future will help to further enhance our understanding of the impacts of lakes on glaciers.

Acknowledgements We would like to thank the reviewers and the editors for their constructive comments and suggestions that improved the quality of this paper.

Author contributions DS: writing-original draft preparation, software, formal analysis. LW: supervision, conceptualization, resources, funding acquisition. AH: resources and writing-review and editing. YW: data curation and writing-review and editing. XG: supervision and resources. MW: software and formal analysis. YZ: software and formal analysis. GK: supervision and writing-review and editing.

Funding This study was supported by the National Natural Science Foundation of China (42275044, 41975081), the CAS "Light of West China" Program (E129030101), the Second Tibetan Plateau Scientific Expedition and Research (STEP) program (2019QZKK0105, 2019QZKK0104), the Scientific Research Foundation of Chengdu University of Information Technology (KYTZ202126) and China Meteorological Administration Innovation and Development Project (CXFZ2021Z036). Georgiy Kirillin was supported by the German Federal Ministry of Education and Research (BMBF, Project ID 01LP2006A) in the framework of the joint Sino-German project IceTMP "Seasonal ice cover on lakes of Qinghai-Tibet and Mongolian

Plateau" and the German Research Foundation (DFG, grant KI 853/16-1).

Data availability All data sets used in this paper are publicly available. The GloboLakes LSWT v4.0 data is available at: https://data.ceda.ac.uk/neodc/globolakes/. The MODIS products and TRMM precipitation data are available at: https://earthdata.nasa.gov/. The ERA5 dataset used in this work is available at: https://www.ecmwf.int/en/forecasts/datasets/reanalysis-datasets/era5. The NCEP-FNL data is available at: https://rda.ucar.edu/datasets/ds083.2/. The GLDBv2 dataset was obtained from the website: http://www.flake.igb-berlin.de/. The daily real-time global sea surface temperature dataset is available at: ftp://polar.ncep.noaa.gov/pub/history/sst/rtg_low_res/.

Declarations

Conflict of interest The authors declare that they have no conflicts of interest.

References

Bibi S, Wang L, Li XP, Zhou J, Chen DL, Yao TD (2018) Climatic and associated cryospheric, biospheric, and hydrological changes on the Tibetan Plateau: a review. Int J Climatol 38:E1–E17. https://doi.org/10.1002/joc.5411

Bolch T, Yao T, Kang S, Buchroithner MF, Scherer D, Maussion F, Huintjes E, Schneider C (2010) A glacier inventory for the western Nyainqentanglha Range and the Nam Co Basin, Tibet, and glacier changes 1976–2009. Cryosphere 4:419–433. https://doi.org/10.5194/tc-4-419-2010

Bonan GB (1995) Sensitivity of a GCM simulation to inclusion of inland water surfaces. J Clim 8:2691–2704. https://doi.org/10.1175/1520-0442(1995)008%3c2691:SOAGST%3e2.0.CO;2

Brun F, Berthier E, Wagnon P, Kaab A, Treichler D (2017) A spatially resolved estimate of High Mountain Asia glacier mass balances from 2000 to 2016. Nat Geosci 10:668. https://doi.org/10.1038/ngeo2999

Cai DL, You QL, Fraedrich K, Guan YN (2017) Spatiotemporal temperature variability over the Tibetan Plateau: altitudinal dependence associated with the global warming hiatus. J Clim 30:969–984. https://doi.org/10.1175/jcli-d-16-0343.1

Cao B, Guan WJ, Li KJ, Wen ZL, Han H, Pan BT (2020) Area and mass changes of glaciers in the West Kunlun mountains based on the analysis of multi-temporal remote sensing images and DEMs from 1970 to 2018. Remote Sensing. https://doi.org/10.3390/rs12162632

Chen F, Dudhia J (2001) Coupling an advanced land surface-hydrology model with the Penn State-NCAR MM5 modeling system. Part II: preliminary model validation. Mon Weather Rev 129:587–604. https://doi.org/10.1175/1520-0493(2001)129%3c0587:Caalsh%3e2.0.Co;2

Chen F, Mitchell K, Schaake J, Xue YK, Pan HL, Koren V, Duan QY, Ek M, Betts A (1996) Modeling of land surface evaporation by four schemes and comparison with FIFE observations. J Geophys Res-Atmos 101:7251–7268. https://doi.org/10.1029/95jd02165

Choulga M, Kourzeneva E, Zakharova E, Doganovsky A (2014) Estimation of the mean depth of boreal lakes for use in numerical weather prediction and climate modelling. Tellus A. https://doi.org/10.3402/tellusa.v66.21295

Da Ronco P, Avanzi F, De Michele C, Notarnicola C, Schaefli B (2020) Comparing MODIS snow products Collection 5 with Collection 6 over Italian Central Apennines. Int J Remote Sens 41:4174–4205. https://doi.org/10.1080/01431161.2020.1714778

de Kok RJ, Tuinenburg OA, Bonekamp PNJ, Immerzeel WW (2018) Irrigation as a potential driver for anomalous glacier behavior in High Mountain Asia. Geophys Res Lett 45:2047–2054. https://doi.org/10.1002/2017gl076158

Dehecq A, Gourmelen N, Gardner AS, Brun F, Goldberg D, Nienow PW, Berthier E, Vincent C, Wagnon P, Trouve E (2019) Twenty-first century glacier slowdown driven by mass loss in High Mountain Asia. Nat Geosci 12:22. https://doi.org/10.1038/s41561-018-0271-9

Deng HJ, Pepin NC, Chen YN (2017) Changes of snowfall under warming in the Tibetan Plateau. J Geophys Res-Atmos 122:7323–7341. https://doi.org/10.1002/2017jd026524

Ding BH, Yang K, Qin J, Wang L, Chen YY, He XB (2014) The dependence of precipitation types on surface elevation and meteorological conditions and its parameterization. J Hydrol 513:154–163. https://doi.org/10.1016/j.jhydrol.2014.03.038

Duan A, Xiao Z (2015) Does the climate warming hiatus exist over the Tibetan Plateau? Sci Rep 5:13711. https://doi.org/10.1038/srep13711

Duan HY, Yao XJ, Liu SY, Gao YP, Qi MM, Liu J, Zhang DH, Li XF (2019) Glacier change in the Tanggula Mountains, Tibetan Plateau, in 1969–2015. J Mt Sci-Engl 16:2663–2678. https://doi.org/10.1007/s11629-018-5011-5

Dudhia J (1989) Numerical study of convection observed during the winter monsoon experiment using a mesoscale two-dimensional model. J Atmos Sci 46:3077–3107. https://doi.org/10.1175/1520-0469(1989)046%3c3077:Nsocod%3e2.0.Co;2

Elvidge AD, Renfrew IA (2016) The causes of foehn warming in the lee of mountains. Bull Am Meteor Soc 97:455–466. https://doi.org/10.1175/Bams-D-14-00194.1

Farinotti D, Immerzeel WW, de Kok RJ, Quincey DJ, Dehecq A (2020) Manifestations and mechanisms of the Karakoram glacier Anomaly. Nat Geosci 13:8. https://doi.org/10.1038/s41561-019-0513-5

Forsythe N, Fowler HJ, Li XF, Blenkinsop S, Pritchard D (2017) Karakoram temperature and glacial melt driven by regional atmospheric circulation variability. Nat Clim Chang 7:664. https://doi.org/10.1038/nclimate3361

Fowler HJ, Archer DR (2006) Conflicting signals of climatic change in the Upper Indus Basin. J Clim 19:4276–4293. https://doi.org/10.1175/jcli3860.1

Fujita K, Nuimura T (2011) Spatially heterogeneous wastage of Himalayan glaciers. Proc Natl Acad Sci USA 108:14011–14014. https://doi.org/10.1073/pnas.1106242108

Gao YH, Leung LR, Zhang YX, Cuo L (2015) Changes in moisture flux over the Tibetan Plateau during 1979–2011: insights from a high-resolution simulation. J Clim 28:4185–4197. https://doi.org/10.1175/Jcli-D-14-00581.1

Gao YH, Chen F, Miguez-Macho G, Li X (2020) Understanding precipitation recycling over the Tibetan Plateau using tracer analysis with WRF. Clim Dyn 55:2921–2937. https://doi.org/10.1007/s00382-020-05426-9

Gerken T, Biermann T, Babel W, Herzog M, Ma Y, Foken T, Graf H-F (2013) A modelling investigation into lake-breeze development and convection triggering in the Nam Co Lake basin, Tibetan Plateau. Theoret Appl Climatol 117:149–167. https://doi.org/10.1007/s00704-013-0987-9

Grell GA, Devenyi D (2002) A generalized approach to parameterizing convection combining ensemble and data assimilation techniques. Geophys Res Lett. https://doi.org/10.1029/2002gl015311

Gu HP, Jin JM, Wu YH, Ek MB, Subin ZM (2015) Calibration and validation of lake surface temperature simulations with the coupled WRF-lake model. Clim Change 129:471–483. https://doi.org/10.1007/s10584-013-0978-y

Guo DL, Wang HJ (2012) The significant climate warming in the northern Tibetan Plateau and its possible causes. Int J Climatol 32:1775–1781. https://doi.org/10.1002/joc.2388

Guo WQ, Liu SY, Xu L, Wu LZ, Shangguan DH, Yao XJ, Wei JF, Bao WJ, Yu PC, Liu Q, Jiang ZL (2015) The second Chinese glacier inventory: data, methods and results. J Glaciol 61:357–372. https://doi.org/10.3189/2015JoG14J209

Hersbach H, Bell B, Berrisford P, Hirahara S, Horányi A, Muñoz-Sabater J, Nicolas J, Peubey C, Radu R, Schepers D, Simmons A, Soci C, Abdalla S, Abellan X, Balsamo G, Bechtold P, Biavati G, Bidlot J, Bonavita M, Chiara G, Dahlgren P, Dee D, Diamantakis M, Dragani R, Flemming J, Forbes R, Fuentes M, Geer A, Haimberger L, Healy S, Hogan RJ, Hólm E, Janisková M, Keeley S, Laloyaux P, Lopez P, Lupu C, Radnoti G, Rosnay P, Rozum I, Vamborg F, Villaume S, Thépaut JN (2020) The ERA5 global reanalysis. Q J R Meteorol Soc 146:1999–2049. https://doi.org/10.1002/qj.3803

Hewitt K (2005) The Karakoram anomaly? Glacier expansion and the "elevation effect", Karakoram Himalaya. Mt Res Dev 25:332–340. https://doi.org/10.1659/0276-4741(2005)025[0332:Tkagea]2.0.Co;2

Hong SY, Lim JOJ (2006) The WRF Single-Moment 6-Class Microphysics Scheme (WSM6). Asia Pacific Journal of Atmospheric Sciences 42:129–151

Hong SY, Noh Y, Dudhia J (2006) A new vertical diffusion package with an explicit treatment of entrainment processes. Mon Weather Rev 134:2318–2341. https://doi.org/10.1175/mwr3199.1

Hostetler SW, Bates GT, Giorgi F (1993) Interactive coupling of a lake thermal-model with a regional climate model. J Geophys Res-Atmos 98:5045–5057. https://doi.org/10.1029/92jd02843

Huffman GJ, Adler RF, Bolvin DT, Gu GJ, Nelkin EJ, Bowman KP, Hong Y, Stocker EF, Wolff DB (2007) The TRMM multisatellite precipitation analysis (TMPA): quasi-global, multiyear, combined-sensor precipitation estimates at fine scales. J Hydrometeorol 8:38–55. https://doi.org/10.1175/Jhm560.1

Hugonnet R, McNabb R, Berthier E, Menounos B, Nuth C, Girod L, Farinotti D, Huss M, Dussaillant I, Brun F, Kaab A (2021) Accelerated global glacier mass loss in the early twenty-first century. Nature 592:726–731. https://doi.org/10.1038/s41586-021-03436-z

Huss M, Bookhagen B, Huggel C, Jacobsen D, Bradley RS, Clague JJ, Vuille M, Buytaert W, Cayan DR, Greenwood G, Mark BG, Milner AM, Weingartner R, Winder M (2017) Toward mountains without permanent snow and ice. Earths Future 5:418–435. https://doi.org/10.1002/2016ef000514

Immerzeel WW, Lutz AF, Andrade M, Bahl A, Biemans H, Bolch T, Hyde S, Brumby S, Davies BJ, Elmore AC, Emmer A, Feng M, Fernández A, Haritashya U, Kargel JS, Koppes M, Kraaijenbrink PDA, Kulkarni AV, Mayewski PA, Nepal S, Pacheco P, Painter TH, Pellicciotti F, Rajaram H, Rupper S, Sinisalo A, Shrestha AB, Viviroli D, Wada Y, Xiao C, Yao T, Baillie JEM (2020) Importance and vulnerability of the world's water towers. Nature 577:364. https://doi.org/10.1038/s41586-019-1822-y

Kanda N, Negi HS, Rishi MS, Kumar A (2020) Performance of various gridded temperature and precipitation datasets over Northwest Himalayan Region. Environ Res Commun. https://doi.org/10.1088/2515-7620/ab9991

Kapnick SB, Delworth TL, Ashfaq M, Malyshev S, Milly PCD (2014) Snowfall less sensitive to warming in Karakoram than in Himalayas due to a unique seasonal cycle. Nat Geosci 7:834–840. https://doi.org/10.1038/Ngeo2269

Kourzeneva E, Asensio H, Martin E, Faroux S (2012) Global gridded dataset of lake coverage and lake depth for use in numerical weather prediction and climate modelling. Tellus A. https://doi.org/10.3402/tellusa.v64i0.15640

Kraaijenbrink PDA, Bierkens MFP, Lutz AF, Immerzeel WW (2017) Impact of a global temperature rise of 1.5 degrees Celsius on Asia's glaciers. Nature 549:257. https://doi.org/10.1038/nature23878

Kuang XX, Jiao JJ (2016) Review on climate change on the Tibetan Plateau during the last half century. J Geophys Res-Atmos 121:3979–4007. https://doi.org/10.1002/2015jd024728

Kumar M, Hodnebrog Ø, Sophie Daloz A, Sen S, Badiger S, Krishnaswamy J (2021) Measuring precipitation in Eastern Himalaya: Ground validation of eleven satellite, model and gauge interpolated gridded products. J Hydrol. https://doi.org/10.1016/j.jhydrol.2021.126252

Li XY, Ma YJ, Huang YM, Hu X, Wu XC, Wang P, Li GY, Zhang SY, Wu HW, Jiang ZY, Cui BL, Liu L (2016) Evaporation and surface energy budget over the largest high-altitude saline lake on the Qinghai-Tibet Plateau. J Geophys Res-Atmos 121:10470–10485. https://doi.org/10.1002/2016jd025027

Li WK, Guo WD, Qiu B, Xue YK, Hsu PC, Wei JF (2018a) Influence of Tibetan Plateau snow cover on East Asian atmospheric circulation at medium-range time scales. Nat Commun 9:9. https://doi.org/10.1038/s41467-018-06762-5

Li XF, Fowler HJ, Forsythe N, Blenkinsop S, Pritchard D (2018b) The Karakoram/Western Tibetan vortex: seasonal and year-to-year variability. Clim Dyn 51:3883–3906. https://doi.org/10.1007/s00382-018-4118-2

Lin H, Li G, Cuo L, Hooper A, Ye QH (2017) A decreasing glacier mass balance gradient from the edge of the Upper Tarim Basin to the Karakoram during 2000–2014. Sci Rep 7:9. https://doi.org/10.1038/s41598-017-07133-8

Loth B, Graf HF (1998) Modeling the snow cover in climate studies - 1. Long-term integrations under different climatic conditions using a multilayered snow-cover model. J Geophys Res-Atmos 103:11313–11327. https://doi.org/10.1029/97jd01411

Luo W, Zhang GQ, Chen WF, Xu FL (2020) Response of glacial lakes to glacier and climate changes in the western Nyainqentanglha range. Sci Total Environ 735:10. https://doi.org/10.1016/j.scitotenv.2020.139607

Ma RH, Yang GS, Duan HT, Jiang JH, Wang SM, Feng XZ, Li AN, Kong FX, Xue B, Wu JL, Li SJ (2010) China's lakes at present: Number, area and spatial distribution. Sci China Earth Sci 54:283–289. https://doi.org/10.1007/s11430-010-4052-6

Ma M, Hui P, Liu D, Zhou P, Tang J (2021) Convection-permitting regional climate simulations over Tibetan Plateau: re-initialization versus spectral nudging. Clim Dyn 58:1719–1735. https://doi.org/10.1007/s00382-021-05988-2

Ma M, Ou T, Liu D, Wang S, Fang J, Tang J (2022) Summer regional climate simulations over Tibetan Plateau: from gray zone to convection permitting scale. Clim Dyn. https://doi.org/10.1007/s00382-022-06314-0

Maussion F, Scherer D, Molg T, Collier E, Curio J, Finkelnburg R (2014) Precipitation seasonality and variability over the Tibetan plateau as resolved by the High Asia Reanalysis. J Clim 27:1910–1927. https://doi.org/10.1175/jcli-d-13-00282.1

Mlawer EJ, Taubman SJ, Brown PD, Iacono MJ, Clough SA (1997) Radiative transfer for inhomogeneous atmospheres: RRTM, a validated correlated-k model for the longwave. J Geophys Res-Atmos 102:16663–16682. https://doi.org/10.1029/97jd00237

Molg T, Maussion F, Scherer D (2014) Mid-latitude westerlies as a driver of glacier variability in monsoonal High Asia. Nat Clim Chang 4:68–73. https://doi.org/10.1038/nclimate2055

Notaro M, Holman K, Zarrin A, Fluck E, Vavrus S, Bennington V (2013) Influence of the Laurentian Great Lakes on regional climate. J Clim 26:789–804. https://doi.org/10.1175/Jcli-D-12-00140.1

Orsolini Y, Wegmann M, Dutra E, Liu BQ, Balsamo G, Yang K, de Rosnay P, Zhu CW, Wang WL, Senan R, Arduini G (2019) Evaluation of snow depth and snow cover over the Tibetan Plateau

in global reanalyses using in situ and satellite remote sensing observations. Cryosphere 13:2221–2239. https://doi.org/10.5194/tc-13-2221-2019

Pepin N, Bradley RS, Diaz HF, Baraer M, Caceres EB, Forsythe N, Fowler H, Greenwood G, Hashmi MZ, Liu XD, Miller JR, Ning L, Ohmura A, Palazzi E, Rangwala I, Schoner W, Severskiy I, Shahgedanova M, Wang MB, Williamson SN, Yang DQ, Mt Res Initiative EDWWG (2015) Elevation-dependent warming in mountain regions of the world. Nat Clim Chang 5:424–430. https://doi.org/10.1038/nclimate2563

Politi E, Maccallum S, Cutler MEJ, Merchant CJ, Rowan JS, Dawson TP (2016) Selection of a network of large lakes and reservoirs suitable for global environmental change analysis using Earth Observation. Int J Remote Sens 37:3042–3060. https://doi.org/10.1080/01431161.2016.1192702

Pritchard HD (2019) Asia's shrinking glaciers protect large populations from drought stress. Nature 569:649. https://doi.org/10.1038/s41586-019-1240-1

Pu ZX, Xu L (2009) MODIS/Terra observed snow cover over the Tibet Plateau: distribution, variation and possible connection with the East Asian Summer Monsoon (EASM). Theor Appl Climatol 97:265–278. https://doi.org/10.1007/s00704-008-0074-9

Qiu J (2008) China: The third pole. Nature 454:393–396. https://doi.org/10.1038/454393a

Sakai A, Fujita K (2017) Contrasting glacier responses to recent climate change in high-mountain Asia. Sci Rep 7:8. https://doi.org/10.1038/s41598-017-14256-5

Samuelsson P, Kourzeneva E, Mironov D (2010) The impact of lakes on the European climate as simulated by a regional climate model. Boreal Environ Res 15:113–129

Scott RW, Huff FA (1996) Impacts of the Great Lakes on regional climate conditions. J Great Lakes Res 22:845–863. https://doi.org/10.1016/S0380-1330(96)71006-7

Shen C, Jia L, Ren S (2022) Inter- and intra-annual glacier elevation change in High Mountain Asia Region based on ICESat-1&2 data using elevation-aspect bin analysis method. Remote Sensing 14:1630

Skamarock WC, Klemp JB, Dudhia J, Gill DO, Barker DM, Wang W, Powers JG (2008) A description of the Advanced Research WRF version 3. NCAR Technical note-475+ STR

Song KS, Wang M, Du J, Yuan Y, Ma JH, Wang M, Mu GY (2016) Spatiotemporal variations of lake surface temperature across the tibetan plateau using MODIS LST product. Remote Sensing 8:20. https://doi.org/10.3390/rs8100854

Su DS, Wen LJ, Gao XQ, Lepparanta M, Song XY, Shi QQ, Kirillin G (2020) Effects of the largest lake of the Tibetan Plateau on the regional climate. J Geophys Res-Atmos. https://doi.org/10.1029/2020JD033396

Subin ZM, Riley WJ, Mironov D (2012) An improved lake model for climate simulations: model structure, evaluation, and sensitivity analyses in CESM1. J Adv Model Earth Syst. https://doi.org/10.1029/2011ms000072

Thiebaux J, Rogers E, Wang WQ, Katz B (2003) A new high-resolution blended real-time global sea surface temperature analysis. Bull Am Meteor Soc 84:645. https://doi.org/10.1175/bams-84-5-645

Thiery W, Davin EL, Panitz HJ, Demuzere M, Lhermitte S, van Lipzig N (2015) The impact of the African Great Lakes on the regional climate. J Clim 28:4061–4085. https://doi.org/10.1175/Jcli-D-14-00565.1

van Angelen JH, Lenaerts JTM, van den Broeke MR, Fettweis X, van Meijgaard E (2013) Rapid loss of firn pore space accelerates 21st century Greenland mass loss. Geophys Res Lett 40:2109–2113. https://doi.org/10.1002/grl.50490

van Pelt WJJ, Pohjola VA, Reijmer CH (2016) The changing impact of snow conditions and refreezing on the mass balance of an Idealized Svalbard Glacier. Front Earth Sci 4:15. https://doi.org/10.3389/feart.2016.00102

Wang QY, Yi S, Chang L, Sun WK (2017) Large-scale seasonal changes in glacier thickness across High Mountain Asia. Geophys Res Lett 44:10427–10435. https://doi.org/10.1002/2017gl075300

Wen LJ, Lv SH, Li ZG, Zhao L, Nagabhatla N (2015) Impacts of the two biggest lakes on local temperature and precipitation in the yellow river source region of the Tibetan Plateau. Adv Meteorol. https://doi.org/10.1155/2015/248031

Wu G (2020) Land-air coupling over the Tibetan Plateau and its climate impacts. Natl Sci Rev 7:485. https://doi.org/10.1093/nsr/nwaa012

Wu KP, Liu SY, Guo WQ, Wei JF, Xu JL, Bao WJ, Yao XJ (2016) Glacier change in the western Nyainqentanglha Range, Tibetan Plateau using historical maps and Landsat imagery: 1970–2014. J Mt Sci-Engl 13:1358–1374. https://doi.org/10.1007/s11629-016-3997-0

Wu SY, Zhang XL, Du JK, Zhou XB, Tuo Y, Li RJ, Duan Z (2019a) The vertical influence of temperature and precipitation on snow cover variability in the Central Tianshan Mountains, Northwest China. Hydrol Process 33:1686–1697. https://doi.org/10.1002/hyp.13431

Wu Y, Huang AN, Yang B, Dong GT, Wen LJ, Lazhu ZZQ, Fu ZP, Zhu XY, Zhang XD, Cai SX (2019b) Numerical study on the climatic effect of the lake clusters over Tibetan Plateau in summer. Clim Dyn 53:5215–5236. https://doi.org/10.1007/s00382-019-04856-4

Yang K, Wu H, Qin J, Lin CG, Tang WJ, Chen YY (2014) Recent climate changes over the Tibetan Plateau and their impacts on energy and water cycle: a review. Glob Planet Change 112:79–91. https://doi.org/10.1016/j.gloplacha.2013.12.001

Yang MX, Wang XJ, Pang GJ, Wang GN, Liu ZC (2019) The Tibetan Plateau cryosphere: observations and model simulations for current status and recent changes. Earth-Sci Rev 190:353–369. https://doi.org/10.1016/j.earscirev.2018.12.018

Yao TD, Thompson L, Mosbrugger V, Zhang F, Ma YM, Luo TX, Xu BQ, Yang XX, Joswiak DR, Wang WC, Joswiak M, Devkota LP, Tayal S, Jilani R, Fayziev R (2012a) Third pole environment (TPE). Environ Dev 3:52–64. https://doi.org/10.1016/j.envdev.2012.04.002

Yao TD, Thompson L, Yang W, Yu WS, Gao Y, Guo XJ, Yang XX, Duan KQ, Zhao HB, Xu BQ, Pu JC, Lu AX, Xiang Y, Kattel DB, Joswiak D (2012b) Different glacier status with atmospheric circulations in Tibetan Plateau and surroundings. Nat Clim Chang 2:663–667. https://doi.org/10.1038/Nclimate1580

Yao TD, Xue YK, Chen DL, Chen FH, Thompson L, Cui P, Koike T, Lau WKM, Lettenmaier D, Mosbrugger V, Zhang RH, Xu BQ, Dozier J, Gillespie T, Gu Y, Kang SC, Piao SL, Sugimoto S, Ueno K, Wang L, Wang WC, Zhang F, Sheng YW, Guo WD, Ailikun YXX, Ma YM, Shen SSP, Su ZB, Chen F, Liang SL, Liu YM, Singh VP, Yang K, Yang DQ, Zhao XQ, Qian Y, Zhang Y, Li Q (2019) Recent third pole's rapid warming accompanies cryospheric melt and water cycle intensification and interactions between monsoon and environment: multidisciplinary approach with observations, modeling, and analysis. Bull Am Meteor Soc 100:423–444. https://doi.org/10.1175/bams-d-17-0057.1

You QL, Zhang YQ, Xie XY, Wu FY (2019) Robust elevation dependency warming over the Tibetan Plateau under global warming of 1.5 degrees C and 2 degrees C. Clim Dyn 53:2047–2060. https://doi.org/10.1007/s00382-019-04775-4

Yu WS, Yao TD, Kang SC, Pu JC, Yang W, Gao TG, Zhao HB, Zhou H, Li SH, Wang WC, Ma LL (2013) Different region climate regimes and topography affect the changes in area and mass balance of glaciers on the north and south slopes of the same glacierized massif (the West Nyainqentanglha Range, Tibetan Plateau). J Hydrol 495:64–73. https://doi.org/10.1016/j.jhydrol.2013.04.034

Yu R, Li J, Zhang Y, Chen H (2015) Improvement of rainfall simulation on the steep edge of the Tibetan Plateau by using a finite-difference transport scheme in CAM5. Clim Dyn 45:2937–2948. https://doi.org/10.1007/s00382-015-2515-3

Zhang QB, Zhang GS (2017) Glacier elevation changes in the western Nyainqentanglha Range of the Tibetan Plateau as observed by TerraSAR-X/TanDEM-X images. Remote Sens Lett 8:1142–1151. https://doi.org/10.1080/2150704x.2017.1362123

Zhang GQ, Yao TD, Xie HJ, Qin J, Ye QH, Dai YF, Guo RF (2014) Estimating surface temperature changes of lakes in the Tibetan Plateau using MODIS LST data. J Geophys Res-Atmos 119:8552–8567. https://doi.org/10.1002/2014jd021615

Zhang ZM, Jiang LM, Liu L, Sun YF, Wang HS (2018) Annual glacier-wide mass balance (2000–2016) of the interior Tibetan plateau reconstructed from MODIS albedo products. Remote Sensing. https://doi.org/10.3390/rs10071031

Zhang C, Tang QH, Chen DL, van der Ent RJ, Liu XC, Li WH, Haile GG (2019a) Moisture source changes contributed to different precipitation changes over the Northern and Southern Tibetan Plateau. J Hydrometeorol 20:217–229. https://doi.org/10.1175/jhm-d-18-0094.1

Zhang GQ, Luo W, Chen WF, Zheng GX (2019b) A robust but variable lake expansion on the Tibetan Plateau. Sci Bull 64:1306–1309. https://doi.org/10.1016/j.scib.2019.07.018

Zhang GQ, Yao TD, Chen WF, Zheng GX, Shum CK, Yang K, Piao SL, Sheng YW, Yi S, Li JL, O'Reilly CM, Qi SH, Shen SSP, Zhang HB, Jia YY (2019c) Regional differences of lake evolution across China during 1960s–2015 and its natural and anthropogenic causes. Remote Sens Environ 221:386–404. https://doi.org/10.1016/j.rse.2018.11.038

Zhang HB, Zhang F, Zhang GQ, Che T, Yan W, Ye M, Ma N (2019d) Ground-based evaluation of MODIS snow cover product V6 across China: Implications for the selection of NDSI threshold. Sci Total Environ 651:2712–2726. https://doi.org/10.1016/j.scitotenv.2018.10.128

Zhang GQ, Yao TD, Xie HJ, Yang K, Zhu LP, Shum CK, Bolch T, Yi S, Allen S, Jiang LG, Chen WF, Ke CQ (2020) Response of Tibetan Plateau lakes to climate change: trends, patterns, and mechanisms. Earth-Sci Rev. https://doi.org/10.1016/j.earscirev.2020.103269

Zhang R, Chan S, Bindlish R, Lakshmi V (2021) Evaluation of global surface water temperature data sets for use in passive remote sensing of soil moisture. Remote Sensing. https://doi.org/10.3390/rs13101872

Zhao Y, Huang AN, Zhou Y, Huang DQ, Yang Q, Ma YF, Li M, Wei G (2014) Impact of the middle and upper tropospheric cooling over Central Asia on the Summer Rainfall in the Tarim Basin, China. J Clim 27:4721–4732. https://doi.org/10.1175/jcli-d-13-00456.1

Zhu ML, Yao TD, Yang W, Xu BQ, Wu GJ, Wang XJ (2017) Differences in mass balance behavior for three glaciers from different climatic regions on the Tibetan Plateau. Clim Dyn 50:3457–3484. https://doi.org/10.1007/s00382-017-3817-4